AWARD NUMBER: W81XWH-18-1-0219

TITLE: Radiogenomic Characterization of Prostate Cancer: Distinguishing Aggressive From Indolent Disease

PRINCIPAL INVESTIGATOR: Simpa S. Salami, MD, MPH

CONTRACTING ORGANIZATION: University of Michigan, Ann Arbor, MI

REPORT DATE: October 2021

TYPE OF REPORT: Annual

PREPARED FOR: U.S. Army Medical Research and Materiel Command
                          Fort Detrick, Maryland 21702-5012

DISTRIBUTION STATEMENT: Approved for Public Release;
                          Distribution Unlimited

The views, opinions and/or findings contained in this report are those of the author(s) and should not be construed as an official Department of the Army position, policy or decision unless so designated by other documentation.

REPORT DOCUMENTATION PAGE			*Form Approved* *OMB No. 0704-0188*

Public reporting burden for this collection of information is estimated to average 1 hour per response, including the time for reviewing instructions, searching existing data sources, gathering and maintaining the data needed, and completing and reviewing this collection of information. Send comments regarding this burden estimate or any other aspect of this collection of information, including suggestions for reducing this burden to Department of Defense, Washington Headquarters Services, Directorate for Information Operations and Reports (0704-0188), 1215 Jefferson Davis Highway, Suite 1204, Arlington, VA 22202-4302. Respondents should be aware that notwithstanding any other provision of law, no person shall be subject to any penalty for failing to comply with a collection of information if it does not display a currently valid OMB control number. **PLEASE DO NOT RETURN YOUR FORM TO THE ABOVE ADDRESS.**

1. REPORT DATE October 2021	2. REPORT TYPE Annual	3. DATES COVERED 30Sep2020-29Sep2021

4. TITLE AND SUBTITLE Radiogenomic Characterization of Prostate Cancer: Distinguishing Aggressive From Indolent Disease	5a. CONTRACT NUMBER W81XWH-18-1-0219
	5b. GRANT NUMBER PC170717
	5c. PROGRAM ELEMENT NUMBER

6. AUTHOR(S): Simpa S. Salami, MD, MPH E-Mail: simpa@umich.edu	5d. PROJECT NUMBER AWD006494
	5e. TASK NUMBER
	5f. WORK UNIT NUMBER

7. PERFORMING ORGANIZATION NAME(S) AND ADDRESS(ES): REGENTS OF THE UNIVERSITY OF MICHIGAN, 503 THOMPSON ST, ANN ARBOR, MI 48109-1340	8. PERFORMING ORGANIZATION REPORT NUMBER

9. SPONSORING / MONITORING AGENCY NAME(S) AND ADDRESS(ES) U.S. Army Medical Research and Development Command Fort Detrick, Maryland 21702-5012	10. SPONSOR/MONITOR'S ACRONYM(S)
	11. SPONSOR/MONITOR'S REPORT NUMBER(S)

12. DISTRIBUTION / AVAILABILITY STATEMENT

Approved for Public Release; Distribution Unlimited

13. SUPPLEMENTARY NOTES
None

14. ABSTRACT: Over the past several years, there has been growing utilization of multi-parametric magnetic resonance imaging (mpMRI) to detect aggressive or high-grade PCa. Even though close to 20 % of aggressive PCa are missed by mpMRI, this imaging modality is currently being used to guide treatment decisions, such as for active surveillance and delineating areas for focal therapy. The goal of this project is to improve the detection of aggressive (Gleason ≥7) PCa by combining mpMRI and urinary biomarkers. Building on our prior work on using PCA3 and TMPRSS2:ERG to detect aggressive PCa, we have developed a novel urine-based targeted next generation sequencing (NGS) assay to detect PCa. We hypothesize that aggressive PCa harbors unique molecular alterations that impact detection by mpMRI or a urine-based sequencing assay. To test this hypothesis, we propose the following Specific Aims: 1): To assess the accuracy of a novel urine-based NGS assay for the detection of high-grade PCa. We will perform targeted DNA/RNA NGS on already collected pre-biopsy post-DRE urine specimens in patients who underwent radical prostatectomy (RP) at the University of Michigan (U-M). The molecular profile of patients with high-grade (cases) versus low-grade (controls) PCa will be compared. 2): To comprehensively characterize the genomic and transcriptomic alterations associated with cancer visibility on mpMRI. We will collect formalin-fixed paraffin-embedded (FFPE) radical prostatectomy (RP) specimens with multiple foci of cancer in men who had mpMRI prior to RP, with an emphasis on those with multiple Gleason grades. Where available, corresponding matched pelvic lymph node specimens with metastasis will also be collected. Targeted multiplexed PCR-based NGS will be performed to characterize and compare the molecular profiles of visible and invisible PCa foci on mpMRI. 3): Determine and compare tissue versus a urine-based prognostic assays to predict upgrading at RP. Targeted DNA/RNA NGS will be performed on post-DRE urine and biopsy tissue obtained prior to RP. We will assess and compare the performance of the novel urine-based assay with tissue-based prognostic assays to predict Gleason upgrading at RP.

15. SUBJECT TERMS None listed.

16. SECURITY CLASSIFICATION OF:			17. LIMITATION OF ABSTRACT	18. NUMBER OF PAGES	19a. NAME OF RESPONSIBLE PERSON USAMRMC
a. REPORT Unclassified	b. ABSTRACT Unclassified	c. THIS PAGE Unclassified	Unclassified	46	19b. TELEPHONE NUMBER *(include area code)*

Standard Form 298 (Rev. 8-98)
Prescribed by ANSI Std. Z39.18

TABLE OF CONTENTS

1. INTRODUCTION:

The goal of this project is to improve the detection of aggressive (Gleason ≥7) prostate cancer by combining multiparametric MRI and urinary biomarkers.

2. KEYWORDS:

Prostate cancer, urinary biomarkers, MRI, aggressive, genomics, transcriptomics

3. ACCOMPLISHMENTS:

What were the major goals of the project?

Major Task 1: Training and educational development in prostate cancer research	1 – 48 Months

Research-Specific Tasks:

Specific Aim 1: To assess the accuracy of a novel urine-based NGS assay for the detection of high-grade PCa.	0 – 20 months
Major Task 1: Test the capacity of a novel urine-based NGS assay to detect aggressive PCa at first biopsy.	0 – 14 months
Major Task 2: Determine the differential performance characteristics of a novel urine-based NGS assay to detect aggressive PCa in the setting of a – vs. + prostate mpMRI.	10 – 20 months
Specific Aim 2: To comprehensively characterize the genomic and transcriptomic alterations associated with cancer visibility on mpMRI	
Major Task 3: Interrogate specific molecular changes associated with high-grade PCa visibility on mpMRI.	16 – 33 months
Major Task 4: Elucidate the molecular profile of low-grade fusion biopsy cores obtained from PIRADS 4 and 5 lesions and correlate these findings with RP pathology.	28 – 38 months
Specific Aim 3: Determine and compare tissue versus a urine-based prognostic assays to predict Gleason upgrading at RP.	
Major Task 5: Assess tissue-based and novel urine-based prognostic scores in biopsy core and urine respectively in patients with Gleason upgrading	34 – 48 months

What was accomplished under these goals?

We continue to make progress in our project specific aims as described below. It is worth mentioning, however, my lab is behind due to the ongoing COVID-19 pandemic and supply chain issues which have severely hampered our planned research activities.

Major Task 1: Training and educational development in prostate cancer research:

Training accomplishments:

- Completion of R01 boot camp program at University of Michigan (UM). This grant writing training program culminated in the submission of an R01 grant application that was reviewed and triaged in June 2020; I revised the grant application based on the reviewer comments and resubmitted in February 2021, discussed and scored but not within fundable range. I will be submitting another grant application in 2022.

- I have continued to attend (virtually) the American Urological Association Annual meetings, Society of Urologic Oncology annual meeting, and Prostate Cancer Foundation annual meetings. I have presented results from this work at some of these meetings. Continue as instructor/faculty of medical school/graduate courses.

- Co-lead of a Prostate SPORE project at UM.

- Awarded the AUA Rising Stars in Urologic Research.

Conferences/journal clubs:
- Attend monthly prostate cancer seminars
- Meet with mentors (Drs. Palapattu and Tomlins) regularly to discuss research progress/career development
  - Continue leadership/active roles in Urology Grand Rounds, GU tumor board, Prostate SPORE collaborative conferences.
- Participated in multiple study sections, including American Cancer Society and American Urological Association. Now standing member of American Cancer Society Committee on Clinical Cancer Research and Epidemiology Study Section.
- Named Review Editor for Urologic Oncology of Frontiers in Urology.

Clinical responsibilities:
- Continue Urologic oncology clinic.
- Continue operative schedules.

Professional accomplishments:
- Member of the AUA and NCCN Prostate Cancer Early Detection guidelines panels. Member of the Society of Nuclear Medicine and Molecular Imaging Appropriateness Use Criteria for PSMA PET imaging in prostate cancer.

Specific Aim 1: To assess the accuracy of a novel urine-based NGS assay for the detection of high-grade PCa.

We published the initial paper describing the Urnie NGS-assay this year. The findings are detailed in:

Cani AK, Hu K, Liu CJ, Siddiqui J, Zheng Y, Han S, Nallandhighal S, Hovelson DH, Xiao L, Pham T, Eyrich NW, Zheng H, Vince R Jr, Tosoian JJ, Palapattu GS, Morgan TM, Wei JT, Udager AM, Chinnaiyan AM, Tomlins SA, **Salami SS.** Development of a Whole-urine, Multiplexed, Next-generation RNA-sequencing Assay for Early Detection of Aggressive Prostate Cancer. Eur Urol Oncol. 2021 Mar 31:S2588-9311(21)00046-8. doi: 10.1016/j.euo.2021.03.002. Online ahead of print.PMID: 33812851

- **Major Task 1:** Test the capacity of a novel urine-based NGS assay to detect aggressive PCa at first biopsy. In the prior progress report, we reported that targeted RNA next generation sequencing (NGS) of urine obtained from patients prior to first biopsy was completed in 170 patients. Initial analyses to develop multiplex models to predict Grade Group (GG2-5) as well as GG3-5 prostate cancers revealed training AUC of 0.63 and 0.70 respectively, which was below our anticipated performance.
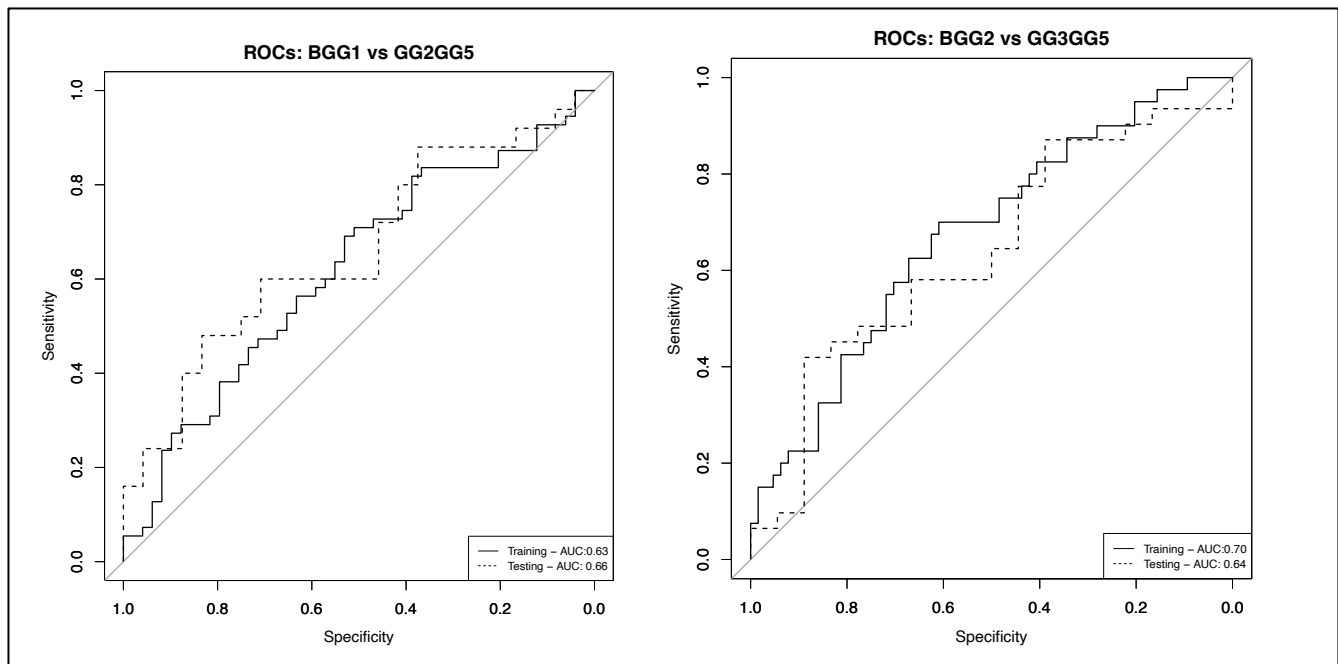
We explored options for potential improvement in the AUC. We found wide variation in the distribution of the transcripts, with some transcripts having poor detection (**Left panel)**. We believe this impacted the performance (measured by AUC) of the resulting models as shown above. Thus, we used a different RNA extraction method from urine in a subset of samples, the Zymo method which requires more urine volume for RNA extraction but takes more time and more hands-on (a manuscript using the Zymo method for RNA extraction is included in this submission). We observed high correlation of most transcripts ($r = 0.75 – 1.0$) between

both RNA extraction methods. However, we also observed poor correlation in some transcripts between the two methods (**Right panel**).
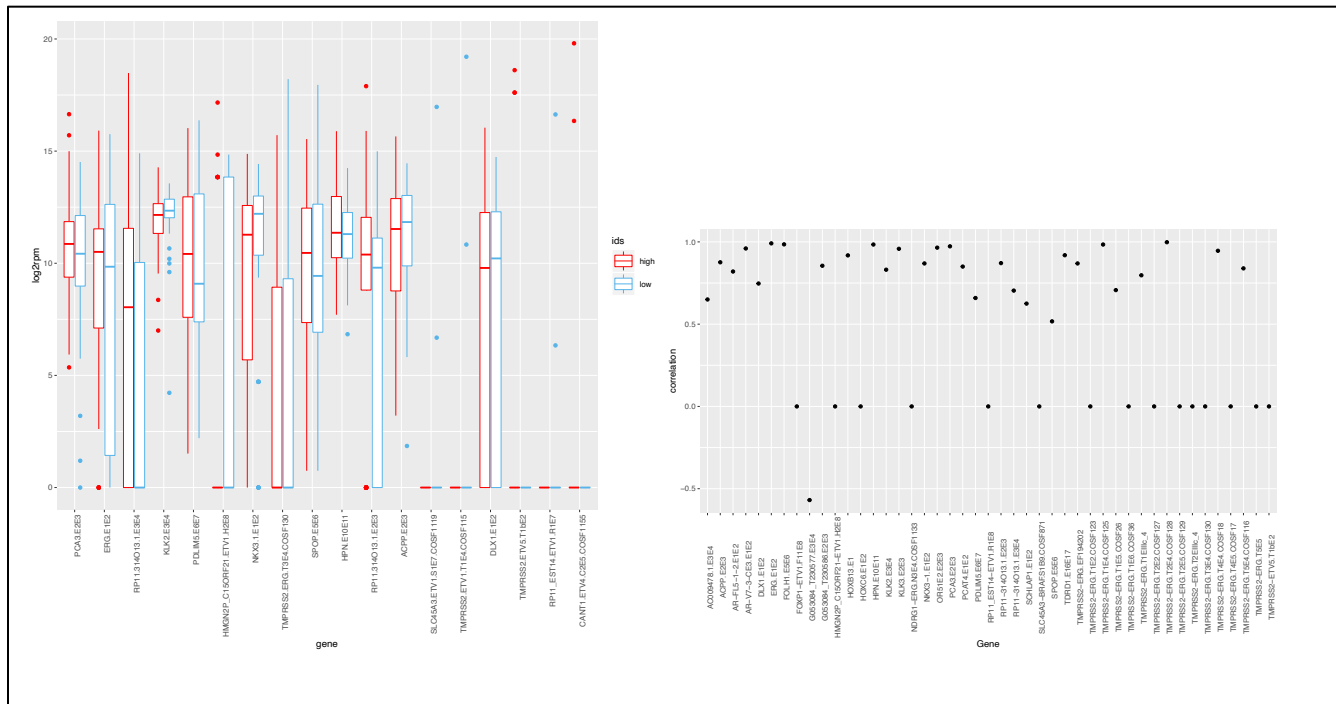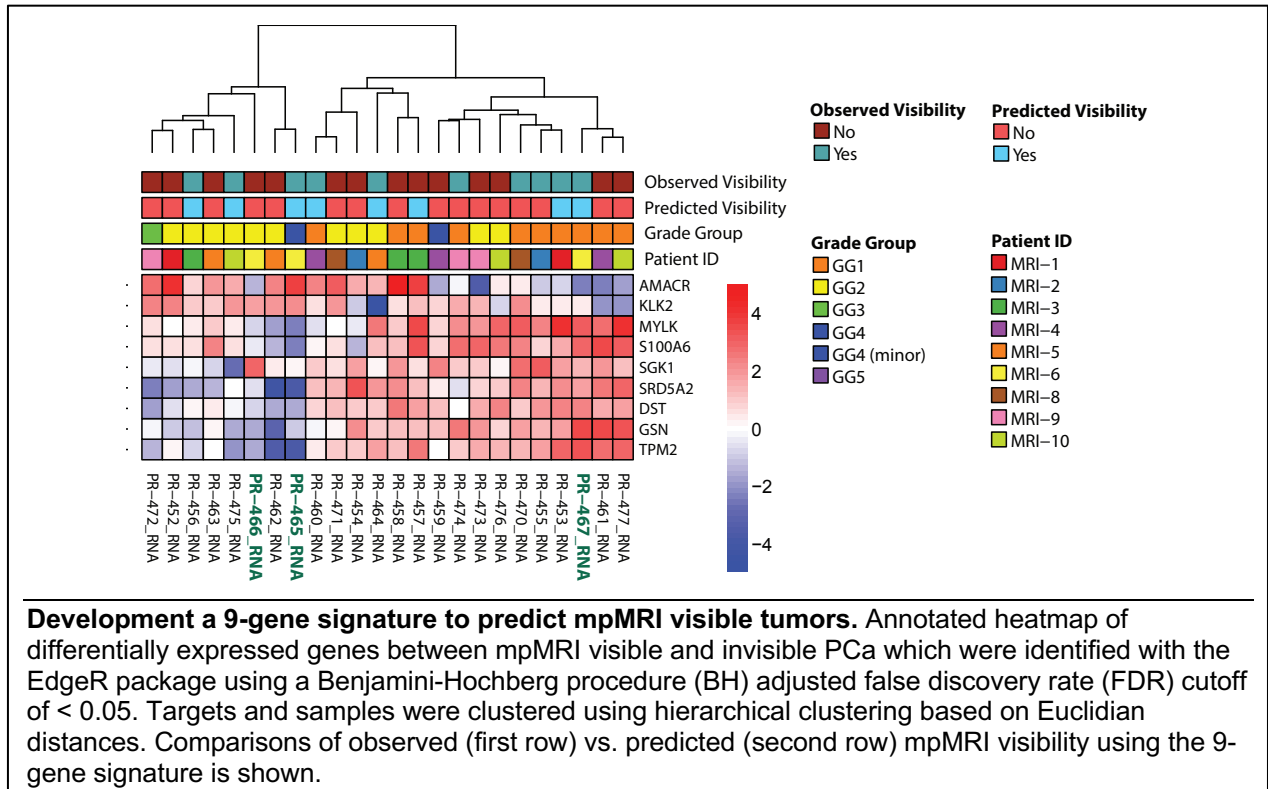

- We have explored the following experimental and analytic approaches:
    - Introduced clinical variables for predicting aggressive disease in model development but with no improvement in performance.
    - Since these experiments were performed on patients who underwent their first prostate biopsies, we are evaluating the possibility of biopsy unersampling as a confounder by collecting follow up biopsy or prostatectomy information to retrain the model.
    - Optimizing RNA extraction in a subset of urine samples with low transcripts detection/expression. Our challenge here was exhaustion of urine specimens given that large volumes of urine was required for RNA extraction using the Zymo method.
    - Earlier this year, our prostate SPORE program in prostate cancer increased the amount of urine collection from patients to accommodate multiple assay comparisons and the goal is to utilize some these specimens in the future to further optimize our assay.

- **Major Task 2: Determine the differential performance characteristics of a novel urine-based NGS assay to detect aggressive PCa in the setting of a – vs. + prostate mpMRI.**
  Next generation sequencing and bioinformatics analysis to evaluate the performance of the novel urine based assay independent of mpMRI in this sub-aim is currently ongoing. This aspect of the study is on hold pending further optimization of our urine assay.

Specific Aim 2: To comprehensively characterize the genomic and transcriptomic alterations associated with cancer visibility on mpMRI

- **Major Task 3: Interrogate specific molecular changes associated with high-grade PCa visibility on mpMRI.**

  We performed <u>targeted NGS</u> in 26 samples of mpMRI visible and invisible prostate cancer. Bioinformatics analysis to compare the molecular profile of mpMRI visible versus invisible lesions indicates that under expression of cellular organization and structure underlies mpMRI invisibility (see publication, **Appendix A)**.

Development a 9-gene signature to predict mpMRI visible tumors. Annotated heatmap of differentially expressed genes between mpMRI visible and invisible PCa which were identified with the EdgeR package using a Benjamini-Hochberg procedure (BH) adjusted false discovery rate (FDR) cutoff of < 0.05. Targets and samples were clustered using hierarchical clustering based on Euclidian distances. Comparisons of observed (first row) vs. predicted (second row) mpMRI visibility using the 9-gene signature is shown.

- We also compared derived commercially available tissue-based prognostic biomarker assays (Myriad Prolaris cell cycle progression (mxCCP), OncotypeDX genomic prostate score (mxGPS), and Decipher genomic classifier (mxGC) between mpMRI visible and invisible lesions and found no significant difference in the scores.
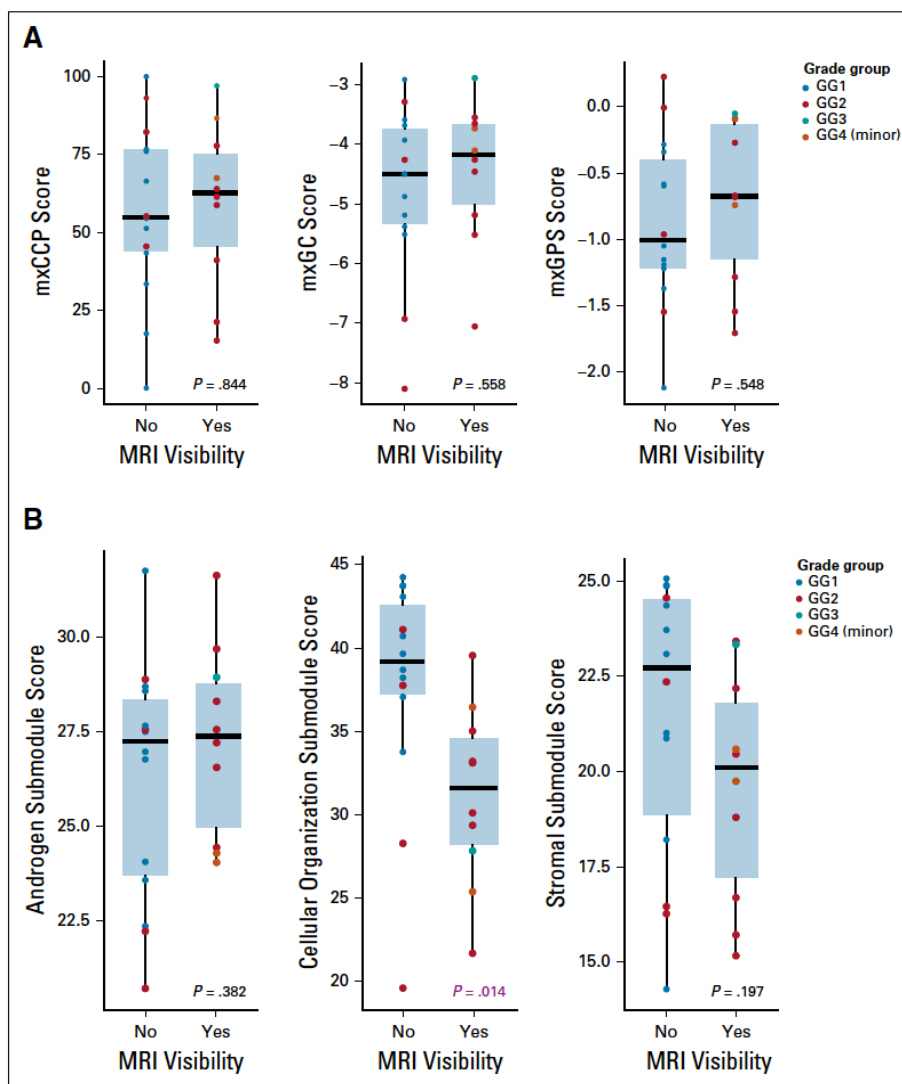
Derivation and comparison of expression-based prognostic scores between mpMRI visible and invisible lesions. A) Boxplots of derived Myriad Prolaris cell cycle progression (mxCCP), OncotypeDX genomic prostate score (mxGPS), and Decipher genomic classifier (mxGC) stratified by mpMRI visibility status in our preliminary cohort (n= 10 patients, 26 cancer foci). Points represent individual cancer focus colored according to ISUP Grade Group. Unpaired t-tests were used to test for significant differences in mean score. There was no statistically significant difference between the derived prognostic scores of mpMRI-visible and - invisible lesions (p > 0.05). **B)** Comparisons of derived mxGPS submodules stratified by mpMRI visibility status. Boxplots of derived mxGPS Androgen, Cellular Organization, and Stromal submodules stratified by mpMRI visibility status are shown. Unpaired t-tests were used to compare mean sub-component scores. Only the Cellular Organization submodule had a significant difference in mean expression (p = 0.014).

- **Major Task 4: Elucidate the molecular profile of low-grade fusion biopsy cores obtained from PIRADS 4 and 5 lesions and correlate these findings with RP pathology.**
  This experiments are ongoing.

- **Major Task 5: Assess tissue-based and novel urine-based prognostic scores in biopsy core and urine respectively in patients with Gleason upgrading**
  This analysis is scheduled to be performed in the 4th year of the award.

What opportunities for training and professional development has the project provided?
Nothing to Report

How were the results disseminated to communities of interest?
Findings were disseminated in the form of publications in journals(Journal of Clinical Oncology Precision Oncology and European Urology Oncology) as well as in talks and interviews.

What do you plan to do during the next reporting period to accomplish the goals?

Major Task 1: Optimize experimental and analytic efforts
- o Optimizing RNA extraction and assay in ongoing urine sample collection.

Major Task 2: Determine the differential performance characteristics of our novel urine-based NGS assay to detect aggressive PCa in the setting of a – vs. + prostate mpMRI. This will be achieved once we optimize our urine RNA extraction.

Major Task 5: Assess tissue-based and novel urine-based prognostic scores in biopsy core and urine respectively in patients with Gleason upgrading. This analysis is scheduled to be performed in the 4th year of the award.

4. **IMPACT:**

What was the impact on the development of the principal discipline(s) of the project?
The finding that mpMRI invisible prostate cancer are just as important biologically as visible ones indicates that we should not use mpMRI alone for determining which patients should undergo focal therapy or active surveillance.

The potential impact of the ongoing analyses will delineate the utility of using a urine test to supplement mpMRI for detecting clinically significant prostate cancer.

What was the impact on other disciplines?
Nothing to report

What was the impact on technology transfer?
Nothing to report

What was the impact on society beyond science and technology?
Nothing to report

5. CHANGES/PROBLEMS:

Changes in approach and reasons for change
See Major task 1 above.

Actual or anticipated problems or delays and actions or plans to resolve them
This project was severely impacted by lab closures and temporary furloughs due to the COVID-19 pandemic. Most recently, we have suffered issues imposed by supply chain shortages. Regarding exhaustion of urine samples necessary for urine RNA extraction optimization, we plan to use ongoing urine sample collection in our prostate cancer SPORE project.

We will need to apply for a no-cost extension of the grant to completed our stated work.

Changes that had a significant impact on expenditures
Nothing to report.

Significant changes in use or care of human subjects, vertebrate animals, biohazards, and/or select agents
Not applicable.

Significant changes in use or care of human subjects
Nothing to report

Significant changes in use or care of vertebrate animals

Not applicable

Significant changes in use of biohazards and/or select agents
Not applicable

6. PRODUCTS:

- **Publications, conference papers, and presentations**

  Journal publications.

  Salami SS, Kaplan JB, Nallandhinghal S, Takhar M, Tosoian JJ, Lee M, Yoon J, Hovelson DH, Plouffe KR, Kaffenberger SD, Schaeffer EM, Karnes R, Lotan TL, Morgan TM, George, AK, Montgomery JS, Davenport MS, You S, Tomlins SA, Curci NE, Kim HL, Spratt DE, Udager AM, Palapattu GS. Biologic Significance of MRI Invisibility in Localized Prostate Cancer (JCO Precision oncology, 2019, in press, acknowledgement of federal support – yes)

  Cani AK, Hu K, Liu CJ, Siddiqui J, Zheng Y, Han S, Nallandhighal S, Hovelson DH, Xiao L, Pham T, Eyrich NW, Zheng H, Vince R Jr, Tosoian JJ, Palapattu GS, Morgan TM, Wei JT, Udager AM, Chinnaiyan AM, Tomlins SA, **Salami SS.** Development of a Whole-urine, Multiplexed, Next-generation RNA-sequencing Assay for Early Detection of Aggressive Prostate Cancer. Eur Urol Oncol. 2021 Mar 31:S2588-9311(21)00046-8. doi: 10.1016/j.euo.2021.03.002. Online ahead of print.PMID: 33812851

  Books or other non-periodical, one-time publications.
  Nothing to report

  Other publications, conference papers and presentations.

  Eyrich NW, Wei JT, Niknafs YS, Siddiqui J, Ellimoottil C, **Salami SS**, Palapattu GS, Mehra R, Kunju LP, Tomlins SA, Chinnaiyan AM, Morgan TM, Tosoian JJ. Association of MyProstateScore (MPS) with prostate cancer grade in the radical prostatectomy specimen. Urol Oncol. 2021 Nov 6:S1078-1439(21)00433-6. doi: 10.1016/j.urolonc.2021.09.007. Online ahead of print.PMID: 34753659

  Stensland KD, Kaffenberger SD, George AK, Morgan TM, Miller DC, **Salami SS**, Dunn RL, Palapattu GS, Montgomery JS, Hollenbeck BK, Skolarus TA. Prostate cancer clinical trial completion: The role of geography. Contemp Clin Trials. 2021 Oct 19;111:106600. doi: 10.1016/j.cct.2021.106600. Online ahead of print.PMID: 34673273

  Jadvar H, Calais J, Fanti S, Feng F, Greene KL, Gulley JL, Hofman M, Koontz BF, Lin DW, Morris MJ, Rowe SP, Royce TJ, **Salami S**, Savir-Baruch B, Srinivas S, Hope TA. Appropriate Use Criteria for Prostate-Specific Membrane Antigen PET Imaging. J Nucl Med. 2021 Sep 30:jnumed.121.263262. doi: 10.2967/jnumed.121.263262. Online ahead of print.PMID: 34593595

  Stangl-Kremser J, Rasul S, Tosoian JJ, **Salami SS**, Zaslavsky A, Udager A, Mazal P, Kain R, Comperat E, Hacker M, Haug A, Mitterhauser M, Pozo-Salido C, Steinbach C, Hassler MR, Kramer G, Shariat SF, Palapattu GS. Single-lesion Prostate-specific

Membrane Antigen Protein Expression (PSMA) and Response to [^{177}Lu]-PSMA-ligand Therapy in Patients with Castration-resistant Prostate Cancer. Eur Urol Open Sci. 2021 Jun 30;30:63-66. doi: 10.1016/j.euros.2021.06.007. eCollection 2021 Aug.PMID: 34337549

Tosoian JJ, Dunn RL, Niknafs YS, Saha A, Vince RA Jr, St Sauver JL, Jacobson DJ, McGree ME, Siddiqui J, Groskopf J, Jacobsen SJ, Tomlins SA, Kunju LP, Morgan TM, **Salami SS**, Wei JT, Chinnaiyan AM, Sarma AV. Association of Urinary MyProstateScore, Age, and Prostate Volume in a Longitudinal Cohort of Healthy Men: Long-term Findings from the Olmsted County Study. Eur Urol Open Sci. 2021 May 25;29:30-35. doi: 10.1016/j.euros.2021.04.009. eCollection 2021 Jul.PMID: 34337531

Shankar PR, Ellimoottil C, George AK, Hadj-Moussa M, Modi PK, **Salami S**, Tosoian JJ, Wei JT, Davenport MS. Testing-Related Health Impact of Transrectal and Transperineal Prostate Biopsy as Assessed by Health Utilities. J Urol. 2021 Dec;206(6):1403-1410. doi: 10.1097/JU.0000000000002118. Epub 2021 Jul 21.PMID: 34288719

Sessine MS, Das S, Park B, **Salami SS**, Kaffenberger SD, Kasputis A, Solorzano M, Luke M, Vince RA, Kaye DR, Borza T, Stoffel EM, Cobain E, Merajver SD, Jacobs MF, Milliron KJ, Caba L, van Neste L, Mondul AM, Morgan TM. Initial Findings from a High Genetic Risk Prostate Cancer Clinic. Urology. 2021 Oct;156:96-103. doi:10.1016/j.urology.2021.05.078. Epub 2021 Jul 17.PMID: 34280438

Cricco-Lizza E, Wilcox Vanden Berg RN, Laviana A, Pantuck M, Basourakos SP, **Salami SS**, Hung AJ, Margolis DJ, Hu JC, McClure TD. Comparative Effectiveness and Tolerability of Transperineal MRI-Targeted Prostate Biopsy under Local versus Sedation. Urology. 2021 Sep;155:33-38. doi: 10.1016/j.urology.2021.06.023. Epub 2021 Jul 2.PMID: 34217762

Gaffney C, Liu D, Cooley V, Ma X, Angulo C, Robinson B, Khani F, Cai P, **Salami S**, Nallandhighal S, Shoag J, Barbieri C. Tumor size and genomic risk in localized prostate cancer. Urol Oncol. 2021 Jul;39(7):434.e17-434.e22. doi: 10.1016/j.urolonc.2021.01.020. Epub 2021 Feb 6.PMID: 33563537

Jairath NK, Dal Pra A, Vince R Jr, Dess RT, Jackson WC, Tosoian JJ, McBride SM, Zhao SG, Berlin A, Mahal BA, Kishan AU, Den RB, Freedland SJ, **Salami SS**, Kaffenberger SD, Pollack A, Tran P, Mehra R, Morgan TM, Weiner AB, Mohamad O, Carroll PR, Cooperberg MR, Karnes RJ, Nguyen PL, Michalski JM, Tward JD, Feng FY, Schaeffer EM, Spratt DE. A Systematic Review of the Evidence for the Decipher Genomic Classifier in Prostate Cancer. Eur Urol. 2021 Mar;79(3):374-383. doi: 10.1016/j.eururo.2020.11.021. Epub 2020 Dec 5.PMID: 33293078 Review.

Tosoian JJ, Trock BJ, Morgan TM, **Salami SS**, Tomlins SA, Spratt DE, Siddiqui J, Kunju LP, Botbyl R, Chopra Z, Pandian B, Eyrich NW, Longton G, Zheng Y, Palapattu GS, Wei JT, Niknafs YS, Chinnaiyan AM. Use of the MyProstateScore Test to Rule Out

[Clinically Significant Cancer: Validation of a Straightforward Clinical Testing Approach.](#) J Urol. 2021 Mar;205(3):732-739. doi: 10.1097/JU.0000000000001430. Epub 2020 Oct 20.PMID: 33080150

Salami SS, Tosoian JJ, Nallandhighal S, Jones TA Jr, Brockman S, Elkhoury FF, Bazzi S, Plouffe KR, Siddiqui J, Liu CJ, Kunju LP, Morgan TM, Natarajan S, Boonstra PS, Sumida L, Tomlins SA, Udager AM, Sisk AE Jr, Marks LS, Palapattu GS. [Serial Molecular Profiling of Low-grade Prostate Cancer to Assess Tumor Upgrading: A Longitudinal Cohort Study.](#) Eur Urol. 2021 Apr;79(4):456-465. doi: 10.1016/j.eururo.2020.06.041. Epub 2020 Jul 3.PMID: 32631746

- **Website(s) or other Internet site(s)**
  https://www.urotoday.com/categories-media/1748-centers-of-excellence/advanced-prostate-cancer-coe/1248-use-of-mri-to-risk-stratify-patients-with-prostate-cancer-simpa-salami.html
  This was an interview with urotoday to discuss the Biologic Significance of Magnetic Resonance Imaging Invisibility in Localized Prostate Cancer.

  https://www.urotoday.com/recent-abstracts/pelvic-health-reconstruction/neurogenic-bladder/1956-video-transcripts/130463-transcript-simpa-salami-recent-eau-article.html
  This was an interview with urotoday to discuss the application of the urine next generation sequencing assay for the detection of aggressive prostate cancer.

- **Technologies or techniques**
  Nothing to report

- **Inventions, patent applications, and/or licenses**
  Nothing to report

- **Other Products**
  Nothing to report

7. PARTICIPANTS & OTHER COLLABORATING ORGANIZATIONS

What individuals have worked on the project?

Name: Simpa S. Salami
Project Role: PI
Researcher Identifier (e.g. ORCID ID): 0000-0001-7461-7079
Nearest person month worked: 6
Contribution to Project: Providing scientific and administrative oversight, data interpretation, manuscript writing
Funding Support: DOD

Name: Sri Nallanghighal, MS
Project Role: Bioinformatician
Researcher Identifier (e.g. ORCID ID):
Nearest person month worked: 4
Contribution to Project: Mr. Nallandhighal has performed bioinformatic analysis of the data generated in Aim 2.
Funding Support: DOD, NIH SPORE

Name: Kevin Hu
Project Role: Graduate Student
Researcher Identifier (e.g. ORCID ID):
Nearest person month worked: 5
Contribution to Project: Mr. Hu has performed bioinformatic analysis of the data generated
Funding Support: UM Department of Pathology Training award

Name: Trinh Pham
Project Role: Laboratory technologist
Researcher Identifier (e.g. ORCID ID):
Nearest person month worked: 5
Contribution to Project: Ms. Pham has performed the laboratory experiments – DNA/RNA extraction from urine and Next generation sequencing
Funding Support: Department of Urology funds

Has there been a change in the active other support of the PD/PI(s) or senior/key personnel since the last reporting period?

Current DOD PRA AWARD

PC170717 (Salami)   10/01/2018-09/30/2022   2.40 Calendar Months
Department of Defense   Source
Country: USA
Annual Directs: Total Award:
Radiogenomic Characterization of Prostate Cancer: Distinguishing Aggressive from Indolent Disease
The successful completion of the proposed project will improve our understanding of the molecular basis of PCa visibility on mpMRI and guide treatment decisions based on mpMRI findings.
Role: PI

Other Awards

P50 CA186786 (Chinnaiyan)   09/01/2019-08/31/2024   1.80 Calendar Months
NIH/NCI   Source
Country: USA
Annual Directs: Total Award:
SPORE Project 2: Michigan Prostate SPORE
The Prostate SPORE program continues to place premiums on rigorous scientific review of its translational research programs, pairing of basic and clinical investigators, drawing on expertise of scientists from within and from outside the prostate cancer field, and utilizing flexibility to fund promising new research approaches.
Role: Co-Lead

AWD017037 (Salami)   01/01/2021-12/31/2024   4.38 Calendar Months
Robert Wood Johnson Foundation   Source
Country: USA
Annual Directs: Total Award
Evolution of Kidney Cancer Metastases: Implications for Surveillance and Targeted Therapy
The goals of this project will define the molecular profile of the kidney cancer clone most likely to metastasize and develop a molecular signature for RCC associated with recurrence/metastasis and/or mortality.
Role: PI

Palapattu (PI)   10/24/2017-06/30/2022   0.01 Calendar Months
Joint Institute for Translational and Clinical Research   Source
Country: USA
Annual Directs: Total Award:
Comprehensive molecular profiling of renal cell carcinoma
The long-term goal of our proposal is to improve the health of men diagnosed with renal cell carcinoma (RCC)
Role: Co-Investigator
*Funds used for lab

16YOUN17 (Salami)   06/27/2016-06/27/2022   0.01 Calendar Months
Prostate Cancer Foundation   Source
Country: USA
Annual Directs: Total Award:

Molecular Characterization of the Biologically Dominant Nodule in Multifocal Prostate Cancer with N1 disease
Goals: To determine and compare the molecular profile of each cancer focus in multifocal prostate cancer; ii) To characterize the biologically dominant nodule or index tumor in multifocal prostate cancer with lymph node (LN) metastasis; and iii) To evaluate the prognostic accuracy of Oncotype DX™, Prolaris™ and Decipher™ scores in predicting LN metastasis.
Role: PI
*Funds used for lab research

<u>PENDING</u>
20-PAF08652 (Zaslavsky)   09/01/2020-08/31/2022   0.12 Calendar Months
Karmanos Cancer Institute/Prostate Cancer Foundation   Source
Country: USA
Annual Directs   Total Award

Tissue and Plasma Biomarker Validation and Refinement and Early Drug Compound Development to Inhibit Pro-inflammatory Cytokines and Chemokines in African and European American Men
We anticipate that validation and refinement of our biomarkers will ultimately be more predictive and independent of clinical outcomes than clinical markers in a future prospective analysis
Role: Co-Investigator

20-PAF08526 (Udager)   06/01/2021-05/31/2024   0.60 Calendar Months
DOD   Source
Country: USA
Annual Directs: Total Award:

Integrative molecular profiling of whole urine in African-American men with aggressive prostate cancer
The goal of this project is to: 1) evaluate the performance of a novel whole urine NGS assay for the detection of high-grade prostate cancer in African-American men; and, 2) validate and apply a high-throughput NGS genomic profiling method for whole urine to identify African-American men with aggressive prostate cancer.
Role: Co-Investigator

21-PAF03379 (Zaslavsky)   07/01/2021-06/30/2024   0.12 Calendar Months
Barbara Ann Karmanos Cancer Institute/NIH   Source
Country: USA
Annual Directs: Total Award:
Tissue and Plasma Biomarker Validation and Refinement and Early Drug Compound Development to Inhibit Pro-inflammatory Cytokines and Chemokines in African and European American Men
We anticipate that validation and refinement of our biomarkers will ultimately be more predictive and independent of clinical outcomes than clinical markers in a future prospective analysis
Role: Co-Investigator

21-PAF01820 (Salami)   09/01/2021-08/31/2026   2.40 Calendar Months

NIH   Source
Country: USA
Annual Directs: Total Award:
Defining the Biological Arc of Grade Group 2 Prostate Cancer
The long-term goal of this project is to improve the early detection of aggressive prostate cancer and reduce racial disparities in this disease
Role: PI

22-PAF02096 (Wang)   09/01/2022-08/31/2026   1.19 calendar months
Penn State/NIH   Source
Country: USA
Annual Directs: Total Award:
Transrectal ultrasound and photoacoustic dual imaging guided biopsy of prostate cancer
Aim 1: Develop and validate a clinical grade transrectal ultrasound and photoacoustic (TRUSPA) system for image- guided targeted biopsy of prostate cancer.
Aim 2: Via the studies on clinically relevant TRAMP mouse model of PCa, develop and validate TRUSPA for PCa detection and grading by quantitatively assessing a list of structural and functional imaging biomarkers.
Aim 3: Via the studies on human subjects, examine the clinical feasibility of TRUSPA, by assessing the imaging biomarkers validated in aim 2, in detecting and grading PCa tumors for guiding needle biopsy.
The team at PSU will take the lead in Aim1 in assembling the clinical grade TRUSPA system, while the proposed studies on animal models in Aim 2 and the experiments on human subjects in Aim 3 will be conducted in parallel at PSU and UM. It is understood by all parties that this is a research project and that the work will be conducted on a best effort basis to achieve these objectives on this time line.
Role: Co-Investigator

OVERLAP
If any of the pending grants are awarded funding will be revised as need be.

What other organizations were involved as partners?
Nothing to report

8. SPECIAL REPORTING REQUIREMENTS

COLLABORATIVE AWARDS: Not applicable

QUAD CHARTS: *Not applicable*

9. APPENDICES:

    a. Appendix A (Published Manuscript): Biologic Significance of Magnetic Resonance Imaging Invisibility in Localized Prostate Cancer.

    b. Appendix B (Published Manuscrupt): Development of a Whole-urine, Multiplexed, Next-generation RNA-sequencing Assay for Early Detection of Aggressive Prostate Cancer.

Biologic Significance of Magnetic Resonance Imaging Invisibility in Localized Prostate Cancer

Simpa S. Salami, MD, MPH[1,2]; Jeremy B. Kaplan[1]; Srinivas Nallandhighal, MS[1]; Mandeep Takhar, MS[3]; Jeffrey J. Tosoian, MD, MPH[1]; Matthew Lee, MD[1]; Junhee Yoon, MS[4]; Daniel H. Hovelson, PhD[1]; Komal R. Plouffe, MS[1]; Samuel D. Kaffenberger, MD[1,2]; Edward M. Schaeffer, MD, PhD[5]; R. Jeffrey Karnes, MD[6]; Tamara L. Lotan, MD[7]; Todd M. Morgan, MD[1,2]; Arvin K. George, MD[1,2]; Jeffrey S. Montgomery, MD, MHSA[1,2]; Matthew S. Davenport, MD[1]; Sungyong You, PhD[4]; Scott A. Tomlins, MD, PhD[1,2]; Nicole E. Curci, MD[1]; Hyung L. Kim, MD[4]; Daniel E. Spratt, MD[2,1]; Aaron M. Udager, MD, PhD[1,2]; and Ganesh S. Palapattu, MD[1,2,8]

abstract

PURPOSE Multiparametric magnetic resonance imaging (mpMRI) is used widely for prostate cancer (PCa) evaluation. Approximately 35% of aggressive tumors, however, are not visible on mpMRI. We sought to identify the molecular alterations associated with mpMRI-invisible tumors and determine whether mpMRI visibility is associated with PCa prognosis.

METHODS Discovery and validation cohorts included patients who underwent mpMRI before radical prostatectomy and were found to harbor both mpMRI-visible (Prostate Imaging and Reporting Data System 3 to 5) and -invisible (Prostate Imaging and Reporting Data System 1 or 2) foci on surgical pathology. Next-generation sequencing was performed to determine differential gene expression between mpMRI-visible and -invisible foci. A genetic signature for tumor mpMRI visibility was derived in the discovery cohort and assessed in an independent validation cohort. Its association with long-term oncologic outcomes was evaluated in a separate testing cohort.

RESULTS The discovery cohort included 10 patients with 26 distinct PCa foci on surgical pathology, of which 12 (46%) were visible and 14 (54%) were invisible on preoperative mpMRI. Next-generation sequencing detected prioritized genetic mutations in 14 (54%) tumor foci (n = 8 mpMRI visible, n = 6 mpMRI invisible). A nine-gene signature (composed largely of cell organization/structure genes) associated with mpMRI visibility was derived (area under the curve = 0.89), and the signature predicted MRI visibility with 75% sensitivity and 100% specificity (area under the curve = 0.88) in the validation cohort. In the testing cohort (n = 375, median follow-up 8 years) there was no significant difference in biochemical recurrence, distant metastasis, or cancer-specific mortality in patients with predicted mpMRI-visible versus -invisible tumors (all $P > .05$).

CONCLUSION Compared with mpMRI-invisible disease, mpMRI-visible tumors are associated with underexpression of cellular organization genes. mpMRI visibility does not seem to be predictive of long-term cancer outcomes, highlighting the need for biopsy strategies that detect mpMRI-invisible tumors.

JCO Precis Oncol. © 2019 by American Society of Clinical Oncology

INTRODUCTION

Distinguishing aggressive from indolent clinically localized prostate cancer (PCa) continues to pose a significant clinical challenge. Recent efforts to overcome this have involved the development and optimization of several diagnostic strategies, including multiparametric magnetic resonance imaging (mpMRI). mpMRI permits visual identification of areas that are suggestive for intermediate to high-grade cancer. The emergence of various MRI/ultrasound fusion biopsy platforms has led to increased detection of aggressive PCa by facilitating targeted biopsy of visible lesions.[1-6] As a result, mpMRI is now widely used in guiding treatment decisions in men with clinically localized disease, especially when selecting patients suitable for active surveillance or potentially focal therapy.[7-10] The prevailing view is that only mpMRI-visible cancers require clinical action.

However, use of mpMRI in the evaluation of men with PCa is limited by cancer multifocality and interfocal disease heterogeneity. Individual patients are known to harbor multiple spatially distinct PCa foci with varying clinical, radiographic, and pathologic characteristics.[11-15] Up to 55% of all PCa foci and 35% of clinically significant foci are not visible on mpMRI.[3,16,17] Furthermore, more than 35% of lesions 1 cm or larger are missed by mpMRI.[17] Although some studies have demonstrated that up to 50% of mpMRI-invisible PCa may harbor relevant genomic alterations, the clinical and prognostic significance of mpMRI-invisible PCa remains unknown.[18] An improved understanding of the molecular characteristics and clinical trajectories of mpMRI-visible and -invisible cancers could facilitate more optimal treatment allocation. For example, if mpMRI-invisible foci are found

CONTEXT

Key Objective

What is the molecular basis for prostate cancer visibility on multiparametric magnetic resonance imaging (mpMRI), and do mpMRI-invisible tumors harbor any clinical or biologic significance compared with visible tumors?

Knowledge Generated

mpMRI-visible tumors demonstrated underexpression of genes associated with cellular organization and structure. Using a novel genetic signature for tumor visibility on mpMRI, patients with predicted mpMRI-visible and -invisible tumors did not experience significant differences in biochemical recurrence, distant metastasis, or cancer-specific mortality during follow-up.

Relevance

Prostate cancers that are mpMRI invisible have similar clinical behavior to mpMRI-visible tumors. Negative mpMRI seems insufficient to rule out clinically relevant prostate cancer, and patients at increased risk should be considered for additional testing or systematic prostate biopsy.

to be biologically indolent, those with a known diagnosis of low-grade disease and a negative mpMRI could be directed toward active surveillance. Similarly, those with a single lesion detected on mpMRI could be more confidently directed toward focal therapy, with low concern for missing a clinically relevant lesion. We herein sought to characterize the molecular profile of mpMRI-visible and -invisible PCa foci using next-generation sequencing (NGS). In addition, we test the prognostic significance of our mpMRI-derived genomic signature after radical prostatectomy (RP).

METHODS

Study Design

The study used three independent patient populations: discovery, validation, and testing cohorts. Institutional review board approval was obtained for each cohort. First, we identified patients with clinically localized disease who underwent preoperative mpMRI at the University of Michigan in 2015 to 2016 and were subsequently found to harbor multifocal PCa at RP. We enriched for patients with both mpMRI visible and invisible PCa (Figs 1A and 1B) to constitute the discovery cohort. The validation cohort from Cedars-Sinai Medical Center included patients with either mpMRI-visible or -invisible foci, as previously described.[19] The testing cohort was composed of patients from the Decipher GRID PCa database treated at Johns Hopkins Medical Institute and Mayo Clinic (ClinicalTrials.gov identifier: NCT02609269) who underwent genome-wide expression profiling after RP.[20,21]

Preoperative Prostate mpMRI and Pathologic Evaluation

In the discovery and validation cohorts, mpMRI comprising T2-weighted imaging, diffusion-weighted imaging, and dynamic contrast-enhanced imaging was obtained. All mpMRI results were re-reviewed and coregistered with whole-mount formalin-fixed paraffin-embedded RP specimens to delineate mpMRI-visible (Prostate Imaging and Reporting Data System [PI-RADS] version 2; score, 3 to 5) and -invisible

foci. Additional procedural details are described in the Data Supplement. Data on mpMRI were not available for the testing cohort.[22]

Targeted DNA and RNA NGS

In the discovery cohort, DNA and RNA from each focus were co-isolated for targeted multiplex NGS as previously described[23] and detailed in the Data Supplement. Our targeted NGS assays were designed to assess relevant PCa genomic and transcriptomic alterations and derive clinically available prognostic tests.[15] The details of RNA sequencing in the validation cohort and genome-wide expression profiling in the testing cohorts have been previously described.[19,24]

Bioinformatic Analysis of the Discovery Cohort

NGS data analysis was performed using Torrent Suite (4.2.0; Thermo Fisher Scientfic, Waltham, MA) and the Coverage Analysis Plug-ins v.5.0.4. (Thermo Fisher Scientific), along with the Ion Reporter (4.2.0; Thermo Fisher Scientific). All other analyses were performed using R Project for Statistical Computing v.3.2.3. Details regarding targeted NGS techniques, quality control parameters, DNA copy number alterations and variant calls, fusion isoform and partner level analysis, androgen receptor (AR) and AR-splice variants detection, and prognostic scores derivation have been previously described and summarized in the Data Supplement.[15,25,26]

Differential Gene Expression Analysis of mpMRI-Visible and -Invisible Cancer Foci

To determine gene expression differences between mpMRI-visible and -invisible tumors, we analyzed RNAseq data from the discovery cohort using two approaches—differential expression (DE) analysis and random forest (RF) classifier—as described in the Data Supplement. From these two approaches, a gene expression signature comprising independent differentially expressed genes was developed to predict mpMRI tumor visibility status.
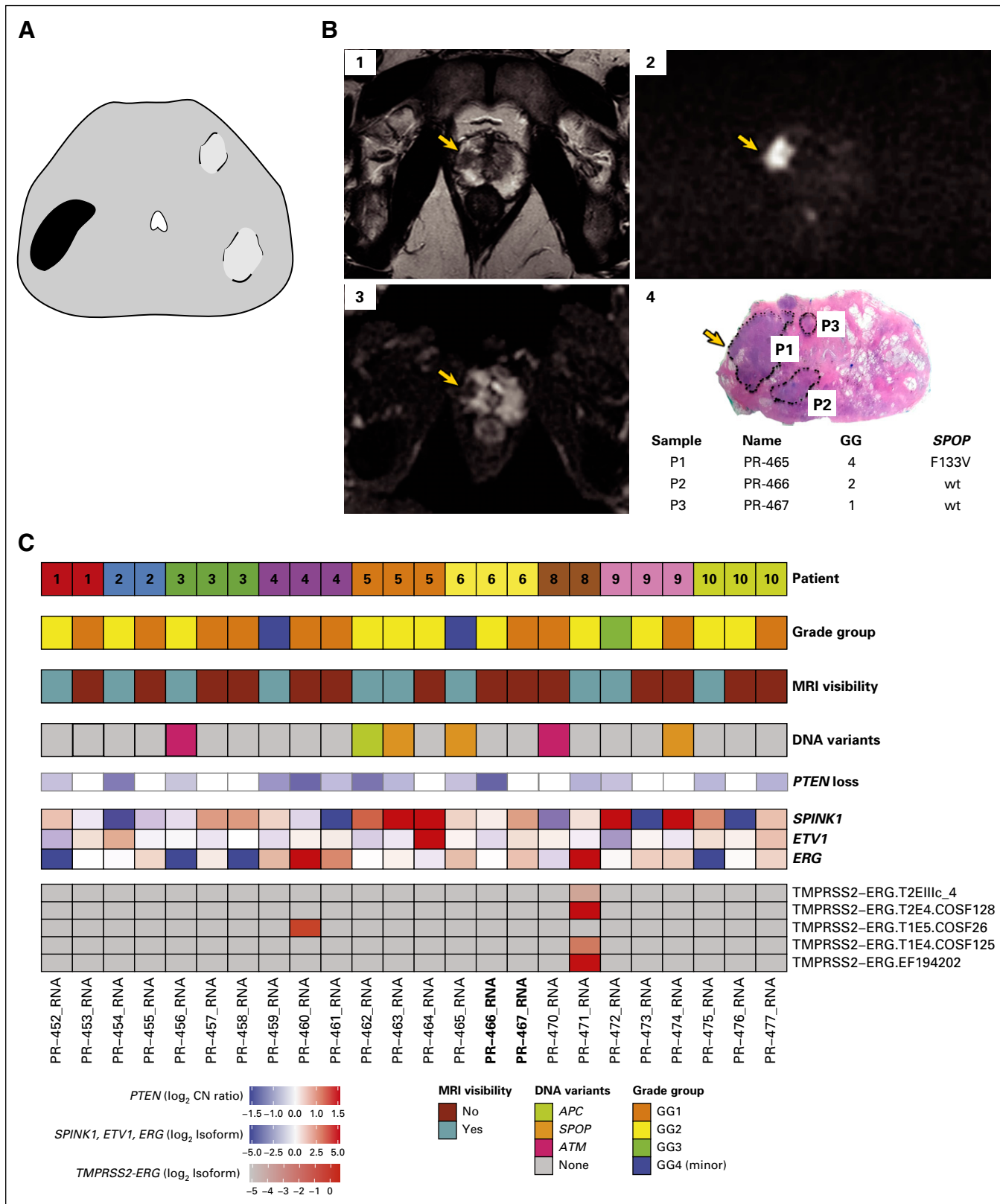
FIG 1. Radiogenomic characterization of multifocal prostate cancer. (A) Cartoon depicting multifocal prostate cancer (PCa) with both multiparametric magnetic resonance imaging (mpMRI)–visible (solid black, left) and invisible (gray with black discontinuous borders, right) lesions. (B) Coregistration of axial mpMRI images with whole-mount histopathology. (1) Axial high-resolution T2, (2) axial diffusion-weighted imaging (*b*-value = 1,600), and (3) axial apparent diffusion coefficient map shows a visible lesion corresponding to cancer focus P1 (grade group [GG] 4; arrows) on the (continued on following page)

Prognostic Significance of mpMRI-Based Gene Expression Signature

A total of 375 patients with genome-wide expression profiles were pooled from two independent case-cohort studies[20,21] to constitute the testing cohort. The mpMRI-based nine-gene expression signature was applied to the testing cohort to predict mpMRI visibility status. Kaplan-Meier curves and Cox proportional hazard regression were used to evaluate the performance of this signature in predicting oncological outcomes: biochemical recurrence-free survival (BFS), distant metastasis–free survival (DMFS), and PCa-specific mortality (PCSM). Multivariable analyses were performed to evaluate this signature as an independent predictor of oncological outcomes after adjusting for relevant clinicopathological variables, including preoperative prostate-specific antigen, pathologic grade group (GG), surgical margins, extraprostatic extension, seminal vesicle invasion, and lymph node invasion. Spearman correlation analysis was performed to measure the association of the gene signature with cellular organization pathway activity. Mean expression of genes involved in the cellular organization pathway on the Oncotype Dx genomic prostate score (GPS; Genomic Health, Redwood City, CA) assay was correlated with the mpMRI-based gene expression signature.[27] Statistical analyses were performed in *R* version 3.3.3, and all statistical tests were two-sided using a .05 significance level.

RESULTS

Study Cohorts

The discovery cohort included 10 patients from the University of Michigan PCa database with both mpMRI-visible and -invisible lesions (Fig 1). The clinicopathological characteristics of the discovery cohort are shown in the Data Supplement. Of the 26 cancer foci identified on surgical pathology specimens, 12 foci (46%) were visible on mpMRI. Among the 14 mpMRI-invisible foci (54%), five (36%) were GG2 and the remainder were GG1 (Fig 1C and Data Supplement). There were 16 patients in the validation cohort, of whom eight (50%) had mpMRI-invisible cancer lesions, and two of these (25%) were GG2 (Data Supplement). A summary of patient-level characteristics of the testing cohort (n = 375) stratified by predicted mpMRI visibility status is shown in the Data Supplement. The median age at RP was 62 years, and median follow-up time for censored patients was 8 years. During follow-up, 136 (36.3%) patients experienced biochemical recurrence,

55 (14.7%) developed metastasis, and 28 (7.5%) died as a result of PCa (Data Supplement).

Detection of Mutations and Copy Number Alterations in the Discovery Cohort

We detected high-confidence mutations in 14 of 26 (54%) tumor foci; six (43%) of the mutations were identified in mpMRI-invisible lesions. Notable somatic point mutations were in *APC*, *ARID1B*, *ATM*, *NOTCH1*, and *SPOP*. We detected *PTEN* one copy number loss in 25% (three of 12) and 14.3% (two of 14) of mpMRI-visible and -invisible foci, respectively (Fig 1C).

Discovery and Validation of a Nine-Gene Expression Signature for mpMRI Visibility

Of the 26 total tumor foci in the discovery cohort and 306 amplicons on the RNAseq panel, 24 samples and 74 amplicons, respectively, passed quality control parameters and underwent DE analysis (Data Supplement). Using DE analysis (Data Supplement) and RF classifier (Data Supplement) to identify candidate differentially expressed genes, we interrogated four separate logistic regression models for predicting mpMRI tumor visibility status using the 19 DE analysis genes, 20 RF genes, 11 shared genes between the DE analysis and RF gene sets, and 11 shared genes combined with the mutually exclusive genes (Data Supplement). A multivariable RNAseq-based logistic regression model with the best performance for predicting mpMRI visibility status, comprising a nine-gene expression signature, was developed from the intersection of the DE analysis and RF gene sets (Fig 2A; Data Supplement). This signature correctly predicted seven (70%) of the mpMRI-visible and 13 (93%) of the mpMRI-invisible foci in the discovery cohort, yielding an area under the curve of 0.89. The optimal probability cutoff for predicting mpMRI-visible tumor was greater than 0.46, with a sensitivity and specificity of 80% and 86%, respectively, in the discovery cohort (Figs 2A and 2B). We observed underexpression of seven of the nine genes in mpMRI-visible tumors, the majority of which were stromal, cellular organization, and structure genes (Fig 2A; Data Supplement).

The nine-gene expression signature was then evaluated in the independent validation cohort (Cedars-Sinai Medical Center) using the predetermined optimal probability cutoff (from the discovery cohort) to predict mpMRI visibility status. The receiver operating characteristic curve in the validation cohort is shown in Fig 2B, with an area under the curve of 0.88. The sensitivity and specificity of the signature

---

FIG 1. (Continued). radical prostatectomy specimen (hematoxylin and eosin, panel 4). Cancer foci P2 (GG 2) and P3 (GG 1) were both mpMRI invisible. (C) Integrative summary of the primary multifocal PCa cohort. Ten patients comprising 26 distinct PCa foci were evaluated. Two samples (patient 7) did not pass initial RNA quality thresholds and were thus omitted. Each patient had at least one MRI-visible and one MRI-invisible cancer focus. Recurrent DNA variants are shown. Log$_2$ copy-number ratio for *PTEN* is also shown. *PTEN* one copy number loss was observed in 25% (three of 12) and 14.3% (two of 14) of mpMRI-visible and invisible cancer foci, respectively (false discovery rate, less than 5%). Expression of *SPINK1*, *ERG*, and *ETV1*, as well as expressed isoforms of *TMPRSS2-ERG* are shown.
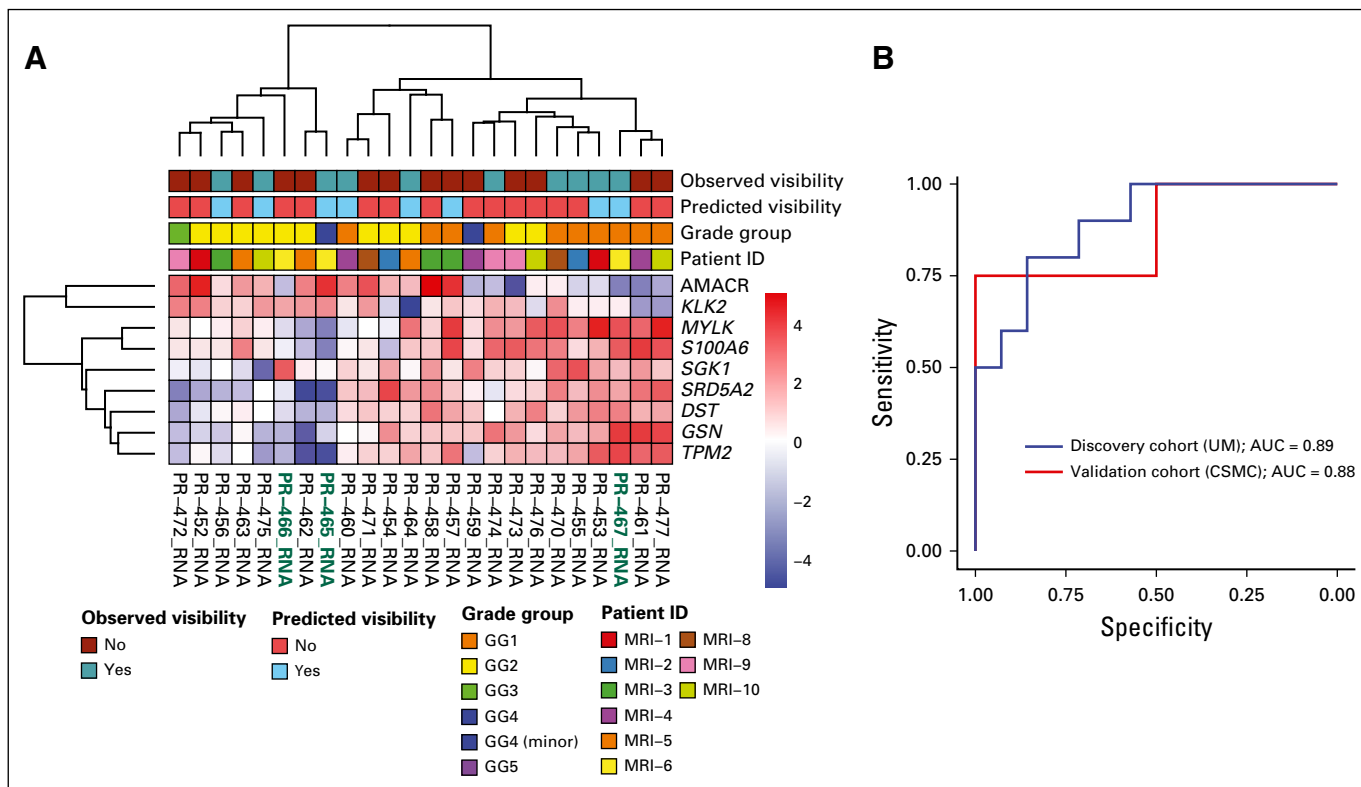
FIG 2. Development and validation of a nine-gene signature to predict multiparametric magnetic resonance imaging (mpMRI)–visible tumors. (A) Annotated heat map of differentially expressed genes in the training cohort. Differentially expressed genes were identified with the EdgeR package using a Benjamini-Hochberg procedure adjusted false discovery rate cutoff of less than 0.05. Targets and samples were clustered using hierarchical clustering on the basis of Euclidian distances. Comparisons of observed (first row) versus predicted (second row) mpMRI visibility using the nine-gene signature are shown in the annotation, as well as International Society of Urological Pathology grade group. (B) Receiver operating characteristic curves for the signature in the discovery (University of Michigan [UM]) versus the validation (Cedars-Sinai Medical Center [CSMC]) cohorts. The signature was developed with multivariable ridge logistic-regression model using cross-validation for λ hyperparameter selection. The area under the curve (AUC) for the signature was not significantly different between the discovery and the validation cohorts (0.89 v 0.88, Delong's unpaired t test, P = .877). The optimal probability cutoff for predicting mpMRI-visible tumor was greater than 0.46, with a sensitivity and specificity of 75% and 100% in the validation cohort, respectively.

for predicting mpMRI visibility status were 75% and 100%, respectively, in the validation cohort. Notably, the signature correctly predicted two GG2 cancers that were mpMRI invisible in the validation cohort.

Prognostic Significance of the Nine-Gene mpMRI Visibility Expression Signature

The distribution of each gene composing the nine-gene signature in the normalized microarray data (testing cohort) from the Decipher GRID mapped to The Cancer Genome Atlas Prostate Adenocarcinoma (TCGA-PRAD) RNAseq closely resemble that of the discovery cohort (Data Supplement). We applied the expression signature to the testing cohort as a proxy for mpMRI tumor visibility. Of the 375 patients in the testing cohort, 177 (47.2%) were classified as mpMRI visible (Data Supplement). Using the predicted probability as a surrogate for mpMRI, we found that the mpMRI visibility signature was not a predictor of BFS, DMFS, or PCSM (Fig 3; all log-rank $P >$ .05). Similar findings were observed when the testing cohort data

were not mapped to the TCGA-PRAD RNAseq cohort (Data Supplement; all log-rank $P >$ .05). Adjusting for relevant clinicopathological variables on multivariable analysis, we found that genomic signature–determined mpMRI visibility status was not an independent predictor of BCR, metastasis, or PCSM (Fig 4; Data Supplement; all $P >$ .05). Similar findings were observed when the testing cohort data were not mapped to the TCGA-PRAD RNAseq data (Data Supplement; all $P >$ .05)

Molecular Basis of Cancer Visibility on mpMRI

Using our multiplex (mx) RNAseq data from the discovery cohort, we derived commercially available tissue-based prognostic biomarker test scores (Myriad Prolaris cell cycle progression [mxCCP] score, Oncotype DX [mxGPS], and the GenomeDX genomic classifier [mxGC]) for each cancer focus, as previously described.[15] We found no significant difference in the mxCCP, mxGPS, and mxGC scores between mpMRI-visible and -invisible foci (Fig 5A; all $P >$ .05). However, as described above, we observed
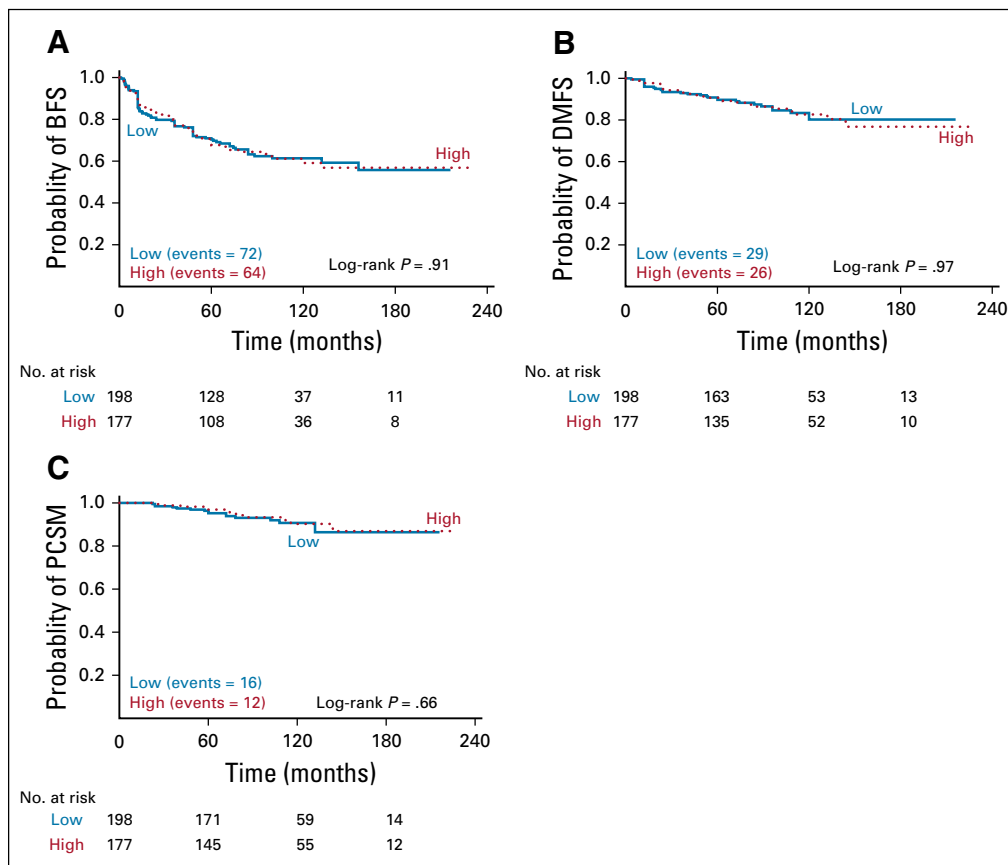
FIG 3. Prognostic significance of predicted multiparametric magnetic resonance imaging (mpMRI) visibility status. Patients (n = 375) in the testing cohort were pooled from two independent case-cohort studies (Johns Hopkins Medical Institute [n = 260] and Mayo Clinic [n = 235]) to test the capacity of predicted mpMRI visibility status to predict (A) biochemical recurrence-free survival (BFS), (B) distant metastasis-free survival (DMFS), and (C) prostate cancer–specific mortality (PCSM). The expression data in this cohort were generated using Affymetrix human exon 1.0 ST array (Santa Clara, CA). Normalization was performed to match the distribution of the genomic data from this cohort to The Cancer Genome Atlas Prostate Adenocarcinoma RNAseq data, as described in Methods, to facilitate testing of the RNASeq-based nine-gene signature to predict mpMRI-visible tumors (Data Supplement). mpMRI visibility status was computed using the signature: high score denotes mpMRI-visible and low score denotes mpMRI-invisible tumor. Kaplan-Meier survival curves were plotted and compared between predicted mpMRI-visible and -invisible tumor using log-rank test. There were no significant differences in BFS, DMFS, and PCSM between predicted mpMRI-visible and -invisible tumors (all $P >$ .05). Similar results were obtained using the Affymetrix microarray data that were not matched to the distribution of the The Cancer Genome Atlas Prostate Adenocarcinoma RNAseq data (Data Supplement).

underexpression of seven of the nine genes in mpMRI-visible tumors, the majority of which were stromal, cellular organization, and structure genes (Fig 2A; Data Supplement). We then computed three subcomponents of the OncotypeDx GPS, as previously described,[15,27] and compared these between mpMRI-visible and -invisible tumors. There were no significant differences in the expression of OncotypeDx GPS androgen signaling and stromal response submodules between mpMRI-visible and -invisible tumors (Fig 5B; both $P >$ .05). However, we found underexpression of the cellular organization submodule of the OncotypeDx GPS panel in mpMRI-visible tumors consistent with the results of the nine-gene signature (Fig 5B; all $P =$ .014).

Similarly, using data from the testing cohort, we found underexpression of the OncotypeDx GPS cellular organization module in predicted mpMRI-visible compared with -invisible foci (Data Supplement; all $P <$ .05). Taken together, these findings suggest that loss of cellular organization and structure contributes to PCa visibility on mpMRI.

DISCUSSION

To better understand the molecular alterations associated with mpMRI visibility and prognostic significance of mpMRI-invisible disease, we performed a comprehensive molecular characterization of primary multifocal PCa inclusive of both mpMRI-visible and -invisible tumor foci
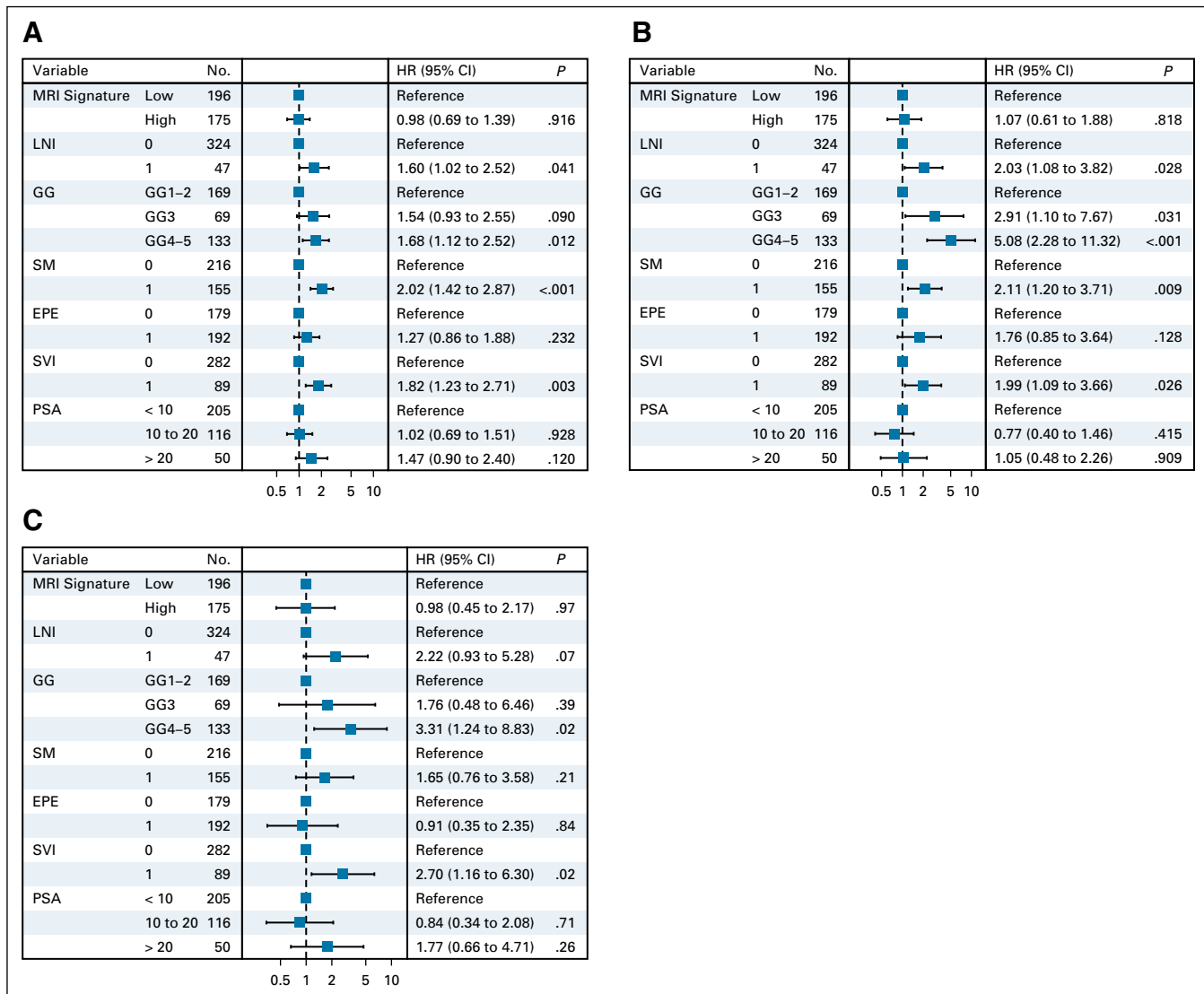
A

Variable		No.		HR (95% CI)	P
MRI Signature	Low	196		Reference	
	High	175		0.98 (0.69 to 1.39)	.916
LNI	0	324		Reference	
	1	47		1.60 (1.02 to 2.52)	.041
GG	GG1–2	169		Reference	
	GG3	69		1.54 (0.93 to 2.55)	.090
	GG4–5	133		1.68 (1.12 to 2.52)	.012
SM	0	216		Reference	
	1	155		2.02 (1.42 to 2.87)	<.001
EPE	0	179		Reference	
	1	192		1.27 (0.86 to 1.88)	.232
SVI	0	282		Reference	
	1	89		1.82 (1.23 to 2.71)	.003
PSA	< 10	205		Reference	
	10 to 20	116		1.02 (0.69 to 1.51)	.928
	> 20	50		1.47 (0.90 to 2.40)	.120

0.5 1 2   5 10

B

Variable		No.		HR (95% CI)	P
MRI Signature	Low	196		Reference	
	High	175		1.07 (0.61 to 1.88)	.818
LNI	0	324		Reference	
	1	47		2.03 (1.08 to 3.82)	.028
GG	GG1–2	169		Reference	
	GG3	69		2.91 (1.10 to 7.67)	.031
	GG4–5	133		5.08 (2.28 to 11.32)	<.001
SM	0	216		Reference	
	1	155		2.11 (1.20 to 3.71)	.009
EPE	0	179		Reference	
	1	192		1.76 (0.85 to 3.64)	.128
SVI	0	282		Reference	
	1	89		1.99 (1.09 to 3.66)	.026
PSA	< 10	205		Reference	
	10 to 20	116		0.77 (0.40 to 1.46)	.415
	> 20	50		1.05 (0.48 to 2.26)	.909

0.5 1 2   5 10

C

Variable		No.		HR (95% CI)	P
MRI Signature	Low	196		Reference	
	High	175		0.98 (0.45 to 2.17)	.97
LNI	0	324		Reference	
	1	47		2.22 (0.93 to 5.28)	.07
GG	GG1–2	169		Reference	
	GG3	69		1.76 (0.48 to 6.46)	.39
	GG4–5	133		3.31 (1.24 to 8.83)	.02
SM	0	216		Reference	
	1	155		1.65 (0.76 to 3.58)	.21
EPE	0	179		Reference	
	1	192		0.91 (0.35 to 2.35)	.84
SVI	0	282		Reference	
	1	89		2.70 (1.16 to 6.30)	.02
PSA	< 10	205		Reference	
	10 to 20	116		0.84 (0.34 to 2.08)	.71
	> 20	50		1.77 (0.66 to 4.71)	.26

0.5 1 2   5 10

FIG 4. Multivariable analysis to assess the prognostic significance of predicted multiparametric magnetic resonance imaging (mpMRI) visibility status. Using data from the testing cohort described in Figure 3 (Affymetrix microarray data matched to the distribution of the The Cancer Genome Atlas Prostate Adenocarcinoma RNAseq data; n = 375), multivariable Cox proportional hazard models were developed to assess the capacity of predicted mpMRI visibility status to predict: (A) biochemical recurrence-free survival (BFS), (B) distant metastasis–free survival (DMFS), and (C) prostate cancer–specific mortality (PCSM), adjusting for relevant clinicopathological variables. mpMRI visibility status was not an independent predictor of BFS, DMFS, and PCSM (all adjusted P > .05). Similar results were obtained when the Affymetrix microarray data were not matched to the distribution of The Cancer Genome Atlas Prostate Adenocarcinoma RNAseq data (Data Supplement). EPE, extraprostatic extension; GG, grade group; HR, hazard ratio; LNI, lymph node invasion; PSA, prostate-specific antigen; SM, surgical margins; SVI, seminal vesical invasion.

using a targeted multiplex NGS approach. We observed that mpMRI-invisible cancer may possess mutations in known cancer-associated genes, with close to 15% harboring *PTEN* one copy number loss. Using robust biostatistic methods, we developed and validated a novel nine-gene signature to predict PCa mpMRI visibility status. Interrogation of this signature in a distinct cohort with long-term follow-up revealed no significant association with BFS, DMFS, or PCSM. Intriguingly, additional analyses revealed that underexpression of genes associated with cellular organization and structure may underpin the molecular

basis of PCa visibility on mpMRI. Taken together, these findings indicate that mpMRI-invisible cancer foci harbor many of the same aggressive molecular features as mpMRI-visible foci and may also be clinically significant.

The molecular basis of PCa visibility on mpMRI is poorly understood. Although tumor size and grade contribute to cancer visibility on mpMRI, the architecture of the glands may play an important role.[28-31] For example, tumors harboring cribriform Gleason pattern 4 were less likely to be detected by mpMRI compared with poorly formed or fused glands, suggesting that tumor size and grade alone do not
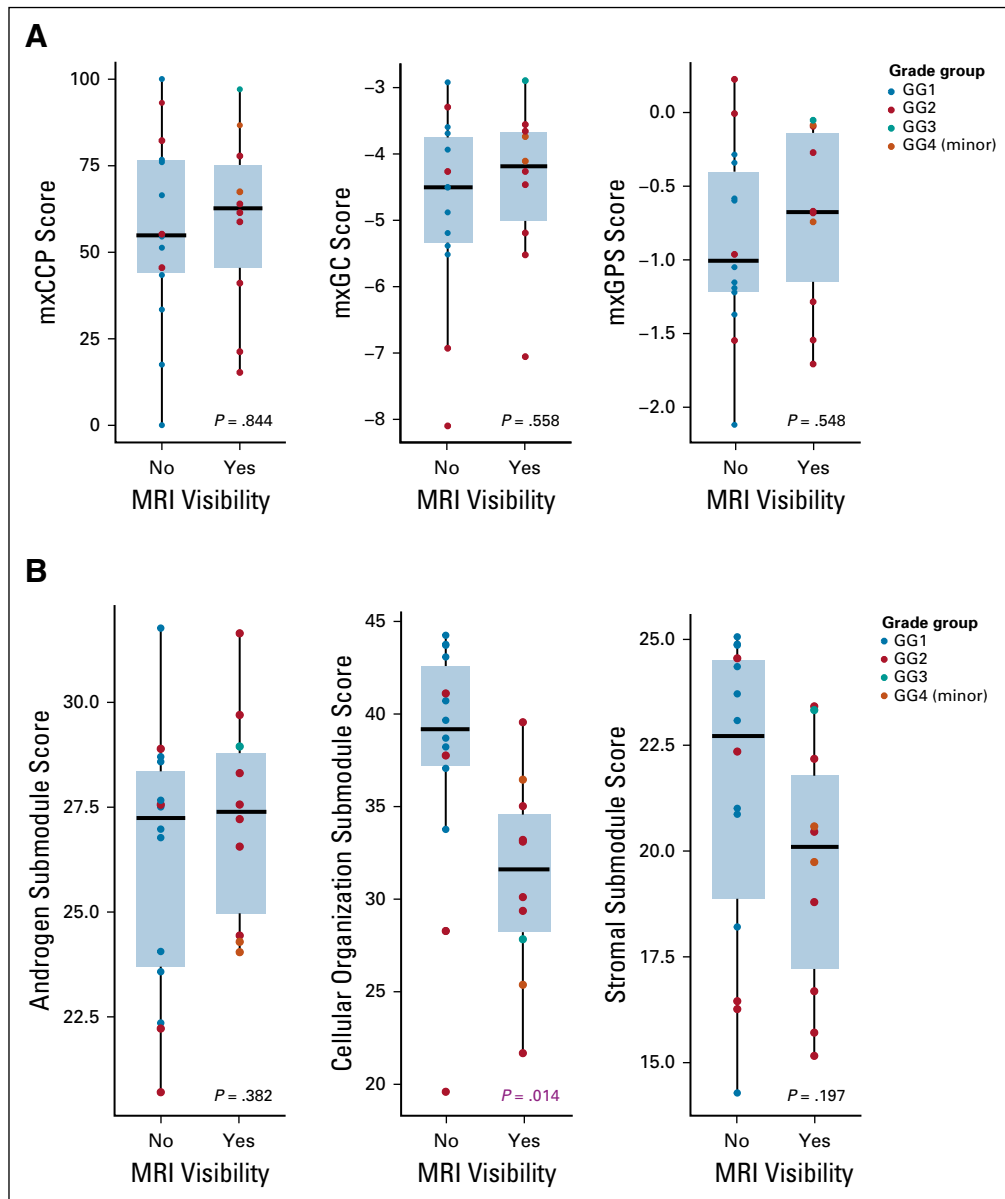
FIG 5. Derivation and comparison of expression-based prognostic scores between multiparametric magnetic resonance imaging (mpMRI)–visible and -invisible lesions. (A) Box plots of derived Prolaris cell cycle progression (mxCCP) score, Oncotype DX genomic prostate score (mxGPS), and Decipher genomic classifier (mxGC) stratified by mpMRI visibility status in the discovery cohort (n = 10 patients; 26 cancer foci). Points represent individual cancer focus colored according to International Society of Urological Pathology grade group (GG). Unpaired *t* tests were used to test for significant differences in mean score. There was no statistically significant difference between the derived prognostic scores of mpMRI-visible and -invisible lesions ($P > .05$). (B) Comparisons of derived mxGPS submodules stratified by mpMRI visibility status. Box plots of derived mxGPS androgen, cellular organization, and stromal submodules stratified by mpMRI visibility status are shown, with each point representing an individual cancer focus colored according to GG. Unpaired *t* tests were used to compare mean subcomponent scores. Only the cellular organization submodule had a significant difference in mean expression ($P = .014$), suggesting that at the RNA expression level mpMRI visibility is related to underlying cellular organization of the tumor.

explain cancer visibility on mpMRI.[28] In a recent report, Li et al[19] observed significant fold changes of differentially expressed genes on the basis of mpMRI visibility regardless of Gleason score or tumor size, including genes involved in cytoskeleton organization. Similarly, the majority of genes composing our novel mpMRI visibility signature are involved in cytoskeletal organization and structure. Other smaller-scale studies have reported the possible role of *CHD1* deletion[32] and *PTEN* loss[33,34] in PCa mpMRI visibility. In the current study, we found that 25% of

mpMRI-visible foci in the discovery cohort demonstrated *PTEN* one copy number loss compared with 14% in mpMRI-invisible foci. In aggregate, our work and that of others suggests that cellular (dis)organization contributes significantly to the underlying basis of PCa visibility on mpMRI. Additional studies are needed to further characterize the fundamental basis of PCa visibility on mpMRI.

The prognostic significance of mpMRI-invisible PCa foci is unknown. Although PCa is multifocal and mpMRI may miss up to 35% of intermediate- to high-grade PCa, the absence of visible lesions on mpMRI has been proposed as a reason to defer confirmatory biopsy when considering active surveillance.[1,3,16,17] In addition, mpMRI is increasingly being used to identify the index or dominant cancer foci for focal therapy. To be sure, although size and grade are believed to be important, how best to define the biologically dominant cancer in multifocal disease is not known.[35] To date, no study has demonstrated the clinical trajectory of mpMRI-visualized lesions. Such a study would be a challenge to perform, given the long duration of follow-up required and the multifocal nature of PCa, with frequent coexistence of mpMRI-visible and -invisible cancers within the same gland.[31]

Salmasi et al[36] reported that the PI-RADS (a grading system for mpMRI lesion visibility) was not a significant predictor of adverse pathology at the time of RP. Similarly, Parry et al[18] found that 50% of mpMRI-invisible cancers harbored one or more genetic alterations commonly observed in metastatic castrate-resistant PCa, suggesting that mpMRI-invisible tumors may be as important as visible ones. In the study by Li et al,[19] a four-gene signature comprising genes differentially expressed between mpMRI-visible and -invisible PCa was shown to predict BFS in two external data sets. However, this signature was not developed as a predictor of or a surrogate for mpMRI cancer visibility, but rather it was selected on the basis of their common association with mpMRI visibility and metastasis. By contrast, in this first study of its kind to our knowledge, using a validated novel mpMRI-based RNAseq signature as a surrogate instrument for mpMRI visibility status, we have demonstrated that predicted mpMRI visibility status was not associated with BFS, DMFS, or PCSM during long-term follow-up. Put another way, mpMRI-invisible PCa does not seem to represent purely indolent disease; mpMRI-invisible lesions may be just as clinically relevant as mpMRI-visible disease. Future studies aimed at better defining the biologically dominant nodule and prognostic significance of mpMRI are warranted.

Our findings have significant clinical implications in the management of PCa. First, in the diagnostic setting, these data corroborate findings from several institutions indicating that a negative mpMRI does not rule out the presence of clinically significant PCa[3,17,31] and should therefore not preclude a prostate biopsy without consideration of clinical risk.[37,38] Second, in the setting of active surveillance, our findings underscore the potential for mpMRI-invisible cancer foci to harbor similar biologic trajectories as mpMRI-visible disease. Although additional studies are needed to delineate the utility of mpMRI in reducing the frequency of surveillance biopsies, the current literature supports systematic in addition to targeted biopsies in men undergoing active surveillance.[3,6] Last, for men considering focal therapy, our data demonstrate that mpMRI alone is not sufficient to rule out the presence of a potentially lethal, nondominant cancer focus.

Our study has several limitations. First, we used a targeted NGS approach; thus it is conceivable that other potential alterations implicated in mpMRI cancer visibility may have been missed. Notwithstanding, our novel RNAseq signature developed from a targeted NGS approach demonstrated high fidelity for predicting mpMRI visibility in the validation cohort, where tumors underwent whole-transcriptome profiling. Second, we did not use the commercially available platforms for Oncotype Dx, Prolaris, and Decipher assays in the discovery cohort. The validity and consistency of deriving these scores from RNAseq data has been previously reported.[15] Third, there were no GG4 and 5 lesions in our cohort. However, our novel RNAseq signature demonstrated high accuracy for predicting mpMRI visibility in the validation cohort, including 19% GG5 lesions. Moreover, GG4 and 5 lesions are generally mpMRI visible, and such patients routinely undergo whole-gland therapy. Fourth, the discovery cohort was made up of a relatively small sample, with low proportion of *ERG*-positive tumors. Nonetheless, we similarly observed high test performance in the validation cohort with ERG overexpression in 31% of samples. Fifth, what constitutes mpMRI-visible or -invisible lesions is not purely objective. To facilitate reproducibility, all lesions in the current study were scored according to the validated PI-RADS v2 system. PI-RADS 1 and 2 lesions were classified as mpMRI invisible, and PI-RADS 3 to 5 were classified as mpMRI visible. Finally, the prognostic significance of mpMRI-invisible cancer was evaluated in the testing cohort using a surrogate molecular marker for mpMRI visibility status. Thus, additional studies are needed to delineate the prognostic significance of mpMRI-invisible PCa in a prospective clinical cohort.

Discerning aggressive from indolent disease remains a significant clinical challenge in the evaluation and management of men with primary PCa. Our findings indicate that mpMRI-invisible cancers were no less likely to harbor lethal biologic potential than visible tumors, highlighting the limitation of using mpMRI alone to guide patient management or delineate specific index cancer foci for ablative therapy. Our results also highlight the continued need for biopsy strategies that detect mpMRI-invisible tumors. Future PCa molecular studies are needed to further characterize the molecular basis of cancer visibility on mpMRI and determine its prognostic significance.

AFFILIATIONS
[1]Michigan Medicine, Ann Arbor, MI
[2]University of Michigan Rogel Cancer Center, Ann Arbor, MI
[3]GenomeDx Biosciences, San Diego, CA
[4]Cedars-Sinai Medical Center, Los Angeles, CA
[5]Northwestern University Feinberg School of Medicine, Chicago, IL
[6]Mayo Clinic, Rochester, MN
[7]Johns Hopkins Medical Institute, Baltimore, MD
[8]Medical University of Vienna, Vienna, Austria

CORRESPONDING AUTHOR
Simpa S. Salami, MD, MPH, Department of Urology, The University of Michigan, 1500 E Medical Center Dr, 7306 RCC/SPC 5948, Ann Arbor, MI 48109-5948; e-mail: simpa@med.umich.edu.

EQUAL CONTRIBUTION
J.B.K., S.N., and M.T. contributed equally to this work; D.E.S., A.M.U., and G.S.P. share co-senior authorship.

AUTHOR CONTRIBUTIONS
Conception and design: Simpa S. Salami, Edward M. Schaeffer, Matthew S. Davenport, Scott A. Tomlins, Daniel E. Spratt, Aaron M. Udager, Ganesh S. Palapattu
Financial support: Scott A. Tomlins, Ganesh S. Palapattu
Administrative support: Ganesh S. Palapattu
Provision of study material or patients: R. Jeffrey Karnes, Arvin K. George, Daniel E. Spratt
Collection and assembly of data: Simpa S. Salami, Jeremy B. Kaplan, Matthew Lee, Komal R. Plouffe, R. Jeffrey Karnes, Tamara L. Lotan, Arvin K. George, Nicole E. Curci, Daniel E. Spratt, Aaron M. Udager
Data analysis and interpretation: Simpa S. Salami, Jeremy B. Kaplan, Srinivas Nallandhighal, Mandeep Takhar, Jeffrey J. Tosoian, Matthew Lee, Junhee Yoon, Daniel H. Hovelson, Samuel D. Kaffenberger, Edward M. Schaeffer, R. Jeffrey Karnes, Todd M. Morgan, Arvin K. George, Jeffrey S. Montgomery, Matthew S. Davenport, Sungyong You, Hyung L. Kim, Daniel E. Spratt, Aaron M. Udager
Manuscript writing: All authors
Final approval of manuscript: All authors

AUTHORS' DISCLOSURES OF POTENTIAL CONFLICTS OF INTEREST
The following represents disclosure information provided by authors of this manuscript. All relationships are considered compensated. Relationships are self-held unless noted. I = Immediate Family Member, Inst = My Institution. Relationships may not relate to the subject matter of this manuscript. For more information about ASCO's conflict of interest policy, please refer to www.asco.org/rwc or ascopubs.org/po/author-center.

Jeremy B. Kaplan
Employment: Tempus Labs

Mandeep Takhar
Employment: GenomeDx

Daniel H. Hovelson
Employment: Strata Oncology
Consulting or Advisory Role: Terumo
Travel, Accommodations, Expenses: Thermo Fisher Scientific

Samuel D. Kaffenberger
Consulting or Advisory Role: MDxHealth, Clovis Oncology
Travel, Accommodations, Expenses: Bristol-Myers Squibb

Edward M. Schaeffer
Consulting or Advisory Role: OPKO Diagnostics, AbbVie

R. Jeffrey Karnes
Research Funding: GenomeDx
Patents, Royalties, Other Intellectual Property: GenomeDx
Travel, Accommodations, Expenses: GenomeDx

Tamara L. Lotan
Consulting or Advisory Role: Janssen Oncology
Research Funding: Ventana Medical Systems

Todd M. Morgan
Consulting or Advisory Role: Myriad Genetics, Terumo BCT
Research Funding: Myriad Genetics (Inst), MDxHealth (Inst), GenomeDx (Inst)

Arvin K. George
Consulting or Advisory Role: Trod Medical
Research Funding: Nanospectra Biosciences (Inst)
Travel, Accommodations, Expenses: Profound Medical, Trod Medical

Matthew S. Davenport
Patents, Royalties, Other Intellectual Property: Royalties from Wolters Kluwer, royalties from uptodate.com

Scott A. Tomlins
Employment: Strata Oncology
Leadership: Strata Oncology
Stock and Other Ownership Interests: Strata Oncology
Consulting or Advisory Role: AbbVie, Janssen, Astellas Medivation, Strata Oncology, Sanofi, Almac Diagnostics
Research Funding: Astellas Medivation (Inst), GenomeDx (Inst)
Patents, Royalties, Other Intellectual Property: I am a coauthor on a patent issued to the University of Michigan on ETS gene fusions in prostate cancer. The diagnostic field of use has been licensed to Hologic/Gen-Probe, who has sublicensed some rights to Ventana Medical Systems/Roche.
Travel, Accommodations, Expenses: Strata Oncology

Hyung L. Kim
Research Funding: GenomeDx
Patents, Royalties, Other Intellectual Property: I am an inventor of a prognostic biomarker signature and immunotherapies.

Daniel E. Spratt
Consulting or Advisory Role: Blue Earth Diagnostics, Janssen Oncology

Aaron M. Udager
Research Funding: Ventana Medical Systems

REFERENCES

1. Kasivisvanathan V, Rannikko AS, Borghi M, et al: MRI-targeted or standard biopsy for prostate-cancer diagnosis. N Engl J Med 378:1767-1777, 2018

2. Ahmed HU, El-Shater Bosaily A, Brown LC, et al: Diagnostic accuracy of multi-parametric MRI and TRUS biopsy in prostate cancer (PROMIS): A paired validating confirmatory study. Lancet 389:815-822, 2017

3. Filson CP, Natarajan S, Margolis DJA, et al: Prostate cancer detection with magnetic resonance-ultrasound fusion biopsy: The role of systematic and targeted biopsies. Cancer 122:884-892, 2016

4. Salami SS, Ben-Levi E, Yaskiv O, et al: In patients with a previous negative prostate biopsy and a suspicious lesion on magnetic resonance imaging, is a 12-core biopsy still necessary in addition to a targeted biopsy? BJU Int 115:562-570, 2015

5. Salami SS, Vira MA, Turkbey B, et al: Multiparametric magnetic resonance imaging outperforms the Prostate Cancer Prevention Trial risk calculator in predicting clinically significant prostate cancer. Cancer 120:2876-2882, 2014

6. Siddiqui MM, Rais-Bahrami S, Turkbey B, et al: Comparison of MR/ultrasound fusion-guided biopsy with ultrasound-guided biopsy for the diagnosis of prostate cancer. JAMA 313:390-397, 2015

7. Ahmed HU, Hindley RG, Dickinson L, et al: Focal therapy for localised unifocal and multifocal prostate cancer: A prospective development study. Lancet Oncol 13:622-632, 2012

8. Natarajan S, Raman S, Priester AM, et al: Focal laser ablation of prostate cancer: Phase I clinical trial. J Urol 196:68-75, 2016

9. Ahmed HU, Dickinson L, Charman S, et al: Focal ablation targeted to the index lesion in multifocal localised prostate cancer: A prospective development study. Eur Urol 68:927-936, 2015

10. Guillaumier S, Peters M, Arya M, et al: A multicentre study of 5-year outcomes following focal therapy in treating clinically significant nonmetastatic prostate cancer. Eur Urol 74:422-429, 2018

11. Boutros PC, Fraser M, Harding NJ, et al: Spatial genomic heterogeneity within localized, multifocal prostate cancer. Nat Genet 47:736-745, 2015

12. Cooper CS, Eeles R, Wedge DC, et al: Analysis of the genetic phylogeny of multifocal prostate cancer identifies multiple independent clonal expansions in neoplastic and morphologically normal prostate tissue. Nat Genet 47:367-372, 2015 [Erratum: Nat Genet 47:689, 2015]

13. Cancer Genome Atlas Research Network: The molecular taxonomy of primary prostate cancer. Cell 163:1011-1025, 2015

14. Kumar A, Coleman I, Morrissey C, et al: Substantial interindividual and limited intraindividual genomic diversity among tumors from men with metastatic prostate cancer. Nat Med 22:369-378, 2016

15. Salami SS, Hovelson DH, Kaplan JB, et al: Transcriptomic heterogeneity in multifocal prostate cancer. JCI Insight 3:123468, 2018

16. Radtke JP, Kuru TH, Boxler S, et al. Comparative analysis of transperineal template saturation prostate biopsy versus magnetic resonance imaging targeted biopsy with magnetic resonance imaging-ultrasound fusion guidance. J Urol 193:87-94, 2015

17. Johnson DC, Raman SS, Mirak SA, et al: Detection of individual prostate cancer foci via multiparametric magnetic resonance imaging. Eur Urol 75:712-720, 2019

18. Parry MA, Srivastava S, Ali A, et al. Genomic evaluation of multiparametric magnetic resonance imaging-visible and -nonvisible lesions in clinically localised prostate cancer. Eur Urol Oncol 2:1-11, 2019

19. Li P, You S, Nguyen C, et al: Genes involved in prostate cancer progression determine MRI visibility. Theranostics 8:1752-1765, 2018

20. Ross AE, Johnson MH, Yousefi K, et al: Tissue-based genomics augments post-prostatectomy risk stratification in a natural history cohort of intermediate- and high-risk men. Eur Urol 69:157-165, 2016

21. Karnes RJ, Bergstralh EJ, Davicioni E, et al: Validation of a genomic classifier that predicts metastasis following radical prostatectomy in an at risk patient population. J Urol 190:2047-2053, 2013

22. Weinreb JC, Barentsz JO, Choyke PL, et al: PI-RADS Prostate Imaging - Reporting and Data System: 2015, Version 2. Eur Urol 69:16-40, 2016

23. Hovelson DH, McDaniel AS, Cani AK, et al: Development and validation of a scalable next-generation sequencing system for assessing relevant somatic variants in solid tumors. Neoplasia 17:385-399, 2015

24. Erho N, Crisan A, Vergara IA, et al: Discovery and validation of a prostate cancer genomic classifier that predicts early metastasis following radical prostatectomy. PLoS One 8:e66855, 2013

25. Warrick JI, Hovelson DH, Amin A, et al: Tumor evolution and progression in multifocal and paired non-invasive/invasive urothelial carcinoma. Virchows Arch 466:297-311, 2015

26. Palapattu GS, Salami SS, Cani AK, et al: Molecular profiling to determine clonality of serial magnetic resonance imaging/ultrasound fusion biopsies from men on active surveillance for low-risk prostate cancer. Clin Cancer Res 23:985-991, 2017

27. Klein EA, Cooperberg MR, Magi-Galluzzi C, et al: A 17-gene assay to predict prostate cancer aggressiveness in the context of Gleason grade heterogeneity, tumor multifocality, and biopsy undersampling. Eur Urol 66:550-560, 2014

28. Truong M, Hollenberg G, Weinberg E, et al: Impact of Gleason subtype on prostate cancer detection using multiparametric magnetic resonance imaging: Correlation with final histopathology. J Urol 198:316-321, 2017

29. Vargas HA, Akin O, Shukla-Dave A, et al: Performance characteristics of MR imaging in the evaluation of clinically low-risk prostate cancer: A prospective study. Radiology 265:478-487, 2012

30. Hurrell SL, McGarry SD, Kaczmarowski A, et al: Optimized *b*-value selection for the discrimination of prostate cancer grades, including the cribriform pattern, using diffusion weighted imaging. J Med Imaging (Bellingham) 5:011004, 2018

31. Le JD, Tan N, Shkolyar E, et al: Multifocality and prostate cancer detection by multiparametric magnetic resonance imaging: Correlation with whole-mount histopathology. Eur Urol 67:569-576, 2015

32. Lee D, Fontugne J, Gumpeni N, et al: Molecular alterations in prostate cancer and association with MRI features. Prostate Cancer Prostatic Dis 20:430-435, 2017

33. McCann SM, Fan X, Wang J, et al: Quantitative multiparametric MRI features and PTEN expression of peripheral zone prostate cancer: A pilot study. 206:559-565, 2016

34. Zundel W, Schindler C, Haas-Kogan D, et al: Loss of PTEN facilitates HIF-1-mediated gene expression. Genes Dev 14:391-396, 2000

35. Haffner MC, Mosbruger T, Esopi DM, et al: Tracking the clonal origin of lethal prostate cancer. J Clin Invest 123:4918-4922, 2013

36. Salmasi A, Khoshnoodi P, Felker ER, et al: A 17-gene genomic prostate score assay provides independent information on adverse pathology in the setting of combined multiparametric magnetic resonance imaging fusion targeted and systematic prostate biopsy. J Urol 200:564-572, 2018

37. Nassiri N, Natarajan S, Margolis DJ, et al: Targeted prostate biopsy: Lessons learned midst the evolution of a disruptive technology. Urology 86:432-438, 2015

38. Panebianco V, Barchetti G, Simone G, et al: Negative multiparametric magnetic resonance imaging for prostate cancer: What's next? Eur Urol 74:48-54, 2018

■-■-■

European Association of Urology

Development of a Whole-urine, Multiplexed, Next-generation RNA-sequencing Assay for Early Detection of Aggressive Prostate Cancer

Q2 *Andi K. Cani* [a,b,c,d], *Kevin Hu* [a,e], *Chia-Jen Liu* [a,c,d], *Javed Siddiqui* [a,c], *Yingye Zheng* [f], *Sumin Han* [a,c], *Srinivas Nallandhighal* [g], *Daniel H. Hovelson* [a,c,e], *Lanbo Xiao* [a,c,d], *Trinh Pham* [g], *Nicholas W. Eyrich* [g], *Heng Zheng* [a,c,d], *Randy Vince Jr* [g], *Jeffrey J. Tosoian* [g], *Ganesh S. Palapattu* [d,g], *Todd M. Morgan* [d,g], *John T. Wei* [a,g], *Aaron M. Udager* [a,c,d], *Arul M. Chinnaiyan* [a,b,c,d,g], *Scott A. Tomlins* [a,b,c,d,g,**], *Simpa S. Salami* [a,d,g,*]

Q3 [a] *Michigan Center for Translational Pathology, University of Michigan Medical School, Ann Arbor, MI, USA;* [b] *Molecular and Cellular Pathology Graduate Program, University of Michigan Medical School, Ann Arbor, MI, USA;* [c] *Department of Pathology, University of Michigan Medical School, Ann Arbor, MI, USA;* [d] *Rogel Cancer Center, University of Michigan, Ann Arbor, MI, USA;* [e] *Department of Computational Medicine and Bioinformatics, University of Michigan Medical School, Ann Arbor, MI, USA;* [f] *Public Health Sciences Division, Fred Hutchinson Cancer Center, Seattle, WA, USA;* [g] *Department of Urology, University of Michigan Medical School, Ann Arbor, MI, USA*

Article info

Abstract

Background: Despite biomarker development advances, early detection of aggressive prostate cancer (PCa) remains challenging. We previously developed a clinical-grade urine test (Michigan Prostate Score [MiPS]) for individualized aggressive PCa risk prediction. MiPS combines serum prostate-specific antigen (PSA), the *TMPRSS2:ERG* (*T2:ERG*) gene fusion, and *PCA3* lncRNA in whole urine after digital rectal examination (DRE).

Objective: To improve on MiPS with a novel next-generation sequencing (NGS) multibiomarker urine assay for early detection of aggressive PCa.

Design, setting, and participants: Preclinical development and validation of a post-DRE urine RNA NGS assay (Urine Prostate Seq [UPSeq]) assessing 84 PCa transcriptomic biomarkers, including *T2:ERG*, *PCA3*, additional PCa fusions/isoforms, mRNAs, lncRNAs, and expressed mutations. Our UPSeq model was trained on 73 patients and validated on a held-out set of 36 patients representing the spectrum of disease (benign to grade group [GG] 5 PCa).

Outcome measurements and statistical analysis: The area under the receiver operating characteristic curve (AUC) of UPSeq was compared with PSA, MiPS, and other existing models/biomarkers for predicting high-grade (GG ≥3) PCa.

Results and limitations: UPSeq demonstrated high analytical accuracy and concordance with MiPS, and was able to detect expressed germline *HOXB13* and somatic *SPOP* mutations. In an extreme design cohort (*n* = 109; benign/GG 1 vs

* Corresponding author. 1500 E. Medical Center Dr. Rm 7306, Ann Arbor, MI 48109, USA.
Tel.: +1 (734) 615-6662; Fax: +1 (734) 647-9840.
E-mail addresses: simpa@med.umich.edu (S.S. Salami).
** Corresponding author. 1500 E. Medical Center Dr. Rm 7420, Ann Arbor, MI 48109, USA.
Tel.: +1 (734)764-1549.
E-mail address: tomlinss@med.umich.edu (S.A. Tomlins).

GG ≥3 PCa, stratified to exclude GG 2 cancer in order to capture signal difference between extreme ends of disease), UPSeq showed differential expression for *T2:ERG.T1E4* (1.2 vs 78.8 median normalized reads, $p < 0.00001$) and *PCA3* (1024 vs 2521, $p = 0.02$), additional *T2:ERG* splice isoforms, and other candidate biomarkers. Using machine learning, we developed a 15-transcript model on the training set ($n = 73$) that outperformed serum PSA and sequencing-derived MiPS in predicting GG ≥3 PCa in the held-out validation set ($n = 36$; AUC 0.82 vs 0.69 and 0.69, respectively).

Conclusions: These results support the potential utility of our novel urine-based RNA NGS assay to supplement PSA for improved early detection of aggressive PCa.

Patient summary: We have developed a new urine-based test for the detection of aggressive prostate cancer, which promises improvement upon current biomarker tests.

© 2021 Published by Elsevier B.V. on behalf of European Association of Urology.

1. Introduction

Despite recent biomarker and imaging advances, noninvasive early detection of aggressive prostate cancer (PCa) remains clinically challenging. Serum prostate-specific antigen (PSA) performance is limited by poor specificity [1], diminishing its utility in early detection of aggressive PCa or active surveillance (AS) of low-risk disease [2,3]. Recently, multiparametric magnetic resonance imaging (mpMRI) has improved the detection of aggressive disease [4]; however, mpMRI misses up to 35% of aggressive PCa foci in multifocal disease [5–7]. Additionally, biopsy remains a costly, complication-prone procedure [8–10]. The current paradigm has led to delayed high-grade PCa detection, unnecessary biopsies, overdetection and overtreatment of likely indolent, low-grade cancer, and unnecessary healthcare expenditure [11]. Hence, accurate noninvasive biomarkers for aggressive PCa are urgently needed.

A urine-based approach has the theoretical potential to overcome PCa multifocality, and inter- and intrafocal heterogeneity [12–14]. Urine provides an opportunity to sample the entire prostate, including lesions missed or undersampled by mpMRI or biopsies. The only Food and Drug Administration–approved PCa urine biomarker test, the PROGENSA PCA3 assay, measures the PCa-associated lncRNA *PCA3* [15]. Other available urine-based laboratory-developed tests (LDTs) include SelectMDx (*DLX1+HOXC6*) [16], the Prostate IntelliScore (*PCA3+ERG*) [17], and Michigan Prostate Score (MiPS; serum PSA + urinary *PCA3* + *TMPRSS2-ERG* [18,19] developed by our group). These tests improve upon PSA alone in predicting the presence of high-grade PCa (grade group [GG] >1). However, the wealth of genomic/transcriptomic information generated in the past decade from tissue-based next-generation sequencing (NGS) studies remains largely underdeveloped as early detection biomarkers [20–23]. None of the currently available urine (or tissue) assays targets gene fusions (beyond TMPRSS2-ERG.T1E4, the predominant fusion transcript isoform joining the first TMPRSS2 exon to the fourth ERG exon) or recurrent germline/somatic mutations, or employs NGS.

Here, we leverage data from PCa genomic and transcriptomic profiling (including our previous development of a 306-gene formalin-fixed paraffin-embedded [FFPE] tissue-based RNA NGS assay [24]) to develop a robust post–digital rectal examination (DRE) whole-urine RNA NGS assay for early detection of aggressive PCa—Urine Prostate Seq (UPSeq). We show high analytical performance of UPSeq, detect germline and somatic PCa driver mutations, and use a machine learning approach to train a preliminary UPSeq model for aggressive PCa detection, which outperformed serum PSA and current models.

2. Patients and methods

2.1. Patient selection, DRE, and urine collection

All samples were collected under institutional review board–approved protocols with informed consent. We retrospectively identified 126 patients to represent the spectrum of disease, benign to GG 5 PCa ($n = 109$ eligible for analyses; Supplementary Table 1 and Supplementary material). Histopathology was assessed based on prostate biopsy ($n = 76$) and radical prostatectomy ($n = 33$). To assess MiPS versus UPSeq concordance, we selected patients with a range of clinical MiPS scores. For UPSeq model development and validation, we used an extreme design strategy, that is, compared benign/GG 1 ($n = 65$) versus GG ≥3 ($n = 44$) PCa. Urine collection was performed after an "attentive" DRE as per the MiPS protocol (see the Supplementary material) [19].

2.2. RNA isolation, UPSeq panel selection, and model development

RNA isolation for UPSeq was performed using the ZR Viral RNA Kit (Supplementary material). Briefly, ~5 ml of urine/GenProbe urine transport media 1:1 mixture was mixed with 3× volume Viral RNA buffer, passed through spin-column filters, washed, and eluted.

A schematic of our computational/experimental strategy is shown in Supplementary Figure 1. A starting pool of 306 target transcripts from our previously developed and validated amplicon-based multiplexed PCa tissue RNAseq panel [24] was filtered down to 84 urine-relevant amplicons, and a custom targeted RNA UPSeq panel was generated by the ThermoFisher "white glove" team for the Ion Torrent AmpliSeq platform.

Targeted NGS was performed as previously described [24–30]. Briefly, 10–15 ng DNase-treated RNA was subjected to random priming reverse

transcription (RT). Target amplification on the cDNA using the UPSeq panel with 23 polymerase chain reaction (PCR) amplification cycles (adjusting up for low-RNA samples) and sequencing was performed on the Ion Torrent platform. Data were analyzed using Torrent Suite 5.0.4. Target end-to-end read numbers were normalized to sample-specific *KLK3* reads. Traditional MiPS was performed as per the protocol [19]. Expressed mutations were analyzed using aligned read pileups in IGV.

Modeling and statistical analysis were performed in R version 3.2.3 (R Foundation for Statistical Computing). We divided the primary extreme design cohort patients (representing the spectrum of disease pathology, excluding GG 2) in a 2:1 ratio for model training and validation, respectively. In the training dataset, we performed variable selection using a random forest-based method and then logistic regression to develop an UPSeq model for predicting GG ≥ 3 disease, maximizing the area under the receiver operating characteristic (AUC) curve. The performance of the final 15-transcript model was evaluated in the extreme design validation set by AUC with 95% confidence interval (CI).

3. Results

3.1. UPSeq assay design

Starting with the 306 transcripts from our previously validated PCa tissue-based RNA NGS assay (Fig. 1) [24], we generated a custom targeted RNA NGS panel (UPSeq) comprising a target set of 84 transcripts (Supplementary Table 2) for urine-based RNA sequencing using the following three criteria: (1) prostate specificity (to avoid confounding urine RNA contributions from other tissues); (2) differential expression in PCa versus normal prostate tissue; and (3) differential expression in aggressive/high-grade PCa versus indolent/low-grade PCa (Fig. 1, violin, box plots). Across a total of 233 samples, we isolated a median of 62.5 ng whole-urine RNA (interquartile range 34.2–109.2 ng) from ~2.5 ml urine with lysis, enough to perform
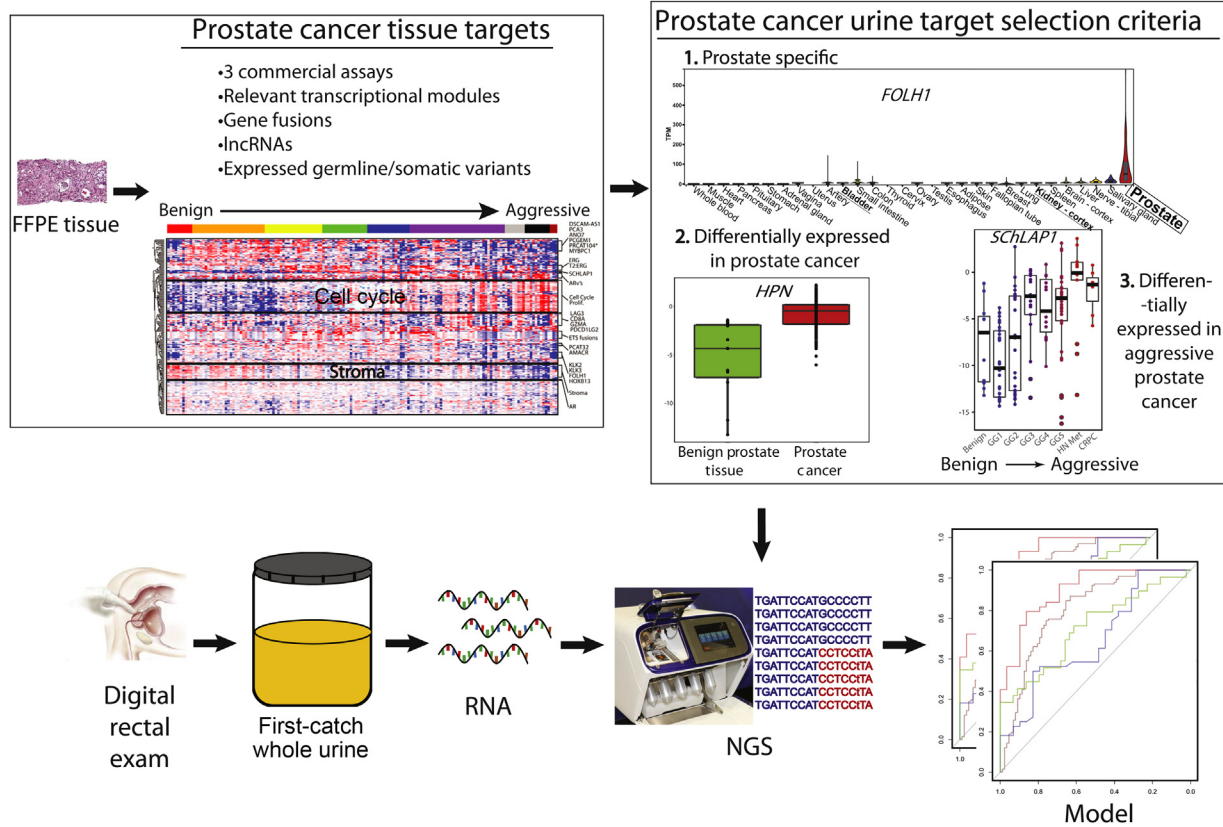
Fig. 1 – Workflow for the development of urine RNA NGS assay (UPSeq) for early detection of aggressive prostate cancer (PCa). Our previously validated FFPE tissue-based PCa prognostic RNA NGS assay [24] served as the starting pool of gene targets and amplicons. Its 306 amplicons include those in the three commercial tissue-based prognostic assays, relevant transcriptional signatures, vast majority of PCa gene fusions, known and novel PCa-related lncRNAs, expressed somatic/germline variants, etc. Heatmap shows tissue expression data with expected patterns of expression across the disease spectrum. We filtered these 306 targets to select 84 transcripts relevant in urine, by prioritizing (1) prostate-specific targets (*FOLH1* expression levels by tissue type in GTEX are shown), (2) transcripts differentially expressed in PCa versus normal prostate tissue (*HPN* tissue expression levels for benign vs prostate cancer are shown [24]), and (3) transcripts differentially expressed in aggressive PCa (grade group >1; *SChLAP1* tissue expression levels for benign vs PCa are shown [24]). For our urine assay, ~30 ml of first-catch urine obtained immediately after a digital rectal examination of the prostate is mixed with RNA-preserving GenProbe urine transport media in a 1:1 ratio. Five milliliters of this mix are used for RNA isolation. NGS with the 84-transcript panel described above is performed on the Ion Torrent sequencing platform, and target transcript read counts are normalized to sample-specific *KLK3* read counts. A machine learning approach was used to train a model for predicting the presence of PCa and aggressive PCa. CRPC = castration-resistant prostate cancer; FFPE = formalin-fixed paraffin embedded; GG = grade group; NGS = next-generation sequencing; UPSeq = Urine Prostate Seq.

UPSeq four times (Supplementary Table 3 and Supplementary material).

3.2.   UPSeq analytical performance and robustness testing

Detailed UPSeq assay analytical performance (Fig. 2 and Supplementary Fig. 2), robustness testing (Supplementary Fig. 3), and compatibility with high-throughput, low-volume urine RNA isolation (Supplementary Fig. 4) are presented in the Supplementary materials.

We performed UPSeq on two replicates each of 10 urine samples performed ~6 mo apart, to mimic real-world conditions and test whether storage affects reproducibility (Fig. 2A). Target transcript expression shown with unsupervised hierarchical clustering yielded highly correlated replicates (median Pearson's R = 0.97, range 0.91–0.99) with a wide dynamic range (representative sample and targets shown in Fig. 2B and 2C). Target correlation matrices yielded expected clusters of related targets (Supplementary Fig. 2). UPSeq also demonstrated high robustness in various suboptimal conditions (Supplementary Fig. 3) and in a high-throughput automated RNA isolation method using ten-fold lower urine input volume (Supplementary Fig. 4). Importantly, we demonstrate the ability of UPSeq to successfully detect a PCa-predisposing HOXB13 p.G84E variant [31,32] in urine RNA of one patient (Supplementary Fig. 5) at 42% variant allele frequency (VAF), potentially a heterozygous germline SNP that was validated in normal matched DNA. UPSeq also successfully detected two SPOP hotspot somatic mutations [20], p.F102C and p.F125I, in two PCa patients (Supplementary Fig. 6 and 7, respectively) at low (but well above background) VAFs (1.62% and 0.42%, respectively), likely due in part to high SPOP expression in normal prostate and urothelium (Supplementary Fig. 8) [33]. Negligible levels of TMPRSS2-ERG reads were present in these samples, consistent with mutual exclusivity between SPOP mutations and ETS gene fusions [20,21]. Taken together, these data support UPSeq's ability to detect expressed PCa predisposing germline variants and somatic mutations in urine, a novel approach in the PCa urinary biomarker field.

We also assessed the performance of UPSeq using whole urine not preceded by DRE (pre-DRE urine), which has implications for direct-to-patient PCa screening. We detected robust pre-DRE levels of highly expressed transcripts (KLK2 and KLK3), concordant with their matched post-DRE samples (R = 0.96 and 0.72, respectively; Supplementary Fig. 9). More modestly expressed transcripts PCA3 and TMPRSS2-ERG.T1E4 were adequately detected, but with generally reduced pre-DRE levels (R = 0.38 and 0.62, respectively). Thus, detection of PCa RNA biomarkers in pre-DRE urine is entirely feasible, even for low-expression genes with some additional optimization.

Finally, to assess assay accuracy against orthogonal methods, we performed reverse transcription quantitative polymerase chain reaction (RT-qPCR) on patient urine RNA samples for PCA3 and the two main TMPRSS2-ERG splicing isoforms (T1E4 and T2E4; Fig. 2D). UPSeq and RT-qPCR expression levels were highly correlated (R = 0.92, 0.95, and 0.97, respectively). Additionally, we assessed the perfor-mance of UPSeq against the transcription-mediated amplification–based MiPS LDT test clinically offered by our group [19]. Standard clinical MiPS scores were highly concordant with UPSeq-derived scores for the two MiPS transcripts (R = 0.75 and 0.96; Fig. 3A and 3B). MiPS also combines these scores with serum PSA into two logistic regression models that predict the risk of PCa or high-grade (GG >1) PCa on pathology [19]. Clinical MiPS versus NGS-derived MiPS model risk predictions were also highly concordant (R = 0.86 vs 0.82) for each model (Fig. 3C and 3D, and Supplementary Table 3). Taken together, these data support UPSeq as a highly reproducible, robust, and accurate assay that recapitulates clinically validated MiPS for quantifying PCa biomarkers in post-DRE urine.

3.3.   UPSeq model training and validation

Of the 126 patients analyzed by UPSeq in our extreme design cohort, data from 109 (86.5%) patients met the stringent sequencing quality criteria to constitute the analytic cohort. It was stratified as 65 men with benign/GG 1 versus 44 men with GG ≥3 cancer, thus excluding GG 2 patients in order to identify any transcriptomic differences between extremes of the disease spectrum, while grouping commonly indolent GG 1 cancer with benign cases. Clinicopathological data showed expected marked differences between the two groups (Supplementary Fig. 10). Conversely, 50/65 (77%) of benign/GG 1 patients had a serum PSA level greater than the commonly used threshold of 4.0 ng/ml, consistent with PSA's modest specificity in this setting.

A number of UPSeq targets showed differential expression between the two groups. Specifically, biomarkers currently (or previously) used in existing clinical urine assays were more highly expressed in urine of higher-GG patients, validating our assay (PCA3 [2521 vs 1024 median normalized reads, p = 0.02], TMPRSS2-ERG.T1E4 [78.8 vs 1.2, p = 0.000003], ERG [955 vs 294, p = 0.0006], TDRD1 [549 vs 128, p = 0.0003], and HOXC6 [0.0 vs 0.0, p = 0.03]), and so were the aggressive PCa-associated lncRNA SChLAP1 (1820 vs 1024, p = 0.005) [34] and a number of additional TMPRSS2-ERG splicing isoforms (Fig. 4A and Supplementary Fig. 11A). T1E4 was the most commonly expressed isoform, followed by T2E4, mirroring PCa tissue (Fig. 4B). Several isoforms were coexpressed in any individual urine sample, with less common ones having lower expression levels, also as previously observed in tissue [24]. Some benign biopsy cases contained low-level urine TMPRSS2-ERG RNA (of the more common isoforms), consistent with the presence of clinically occult cancer foci missed by random systematic or even MRI-guided biopsy [6,24]. Importantly, higher-grade cancers expressed rarer isoforms such as T1EIIIc_4 and T2EIIIc_4, which were at least not detectably present in benign/low-grade cases (Fig. 4B). Taken together, this suggests potential utility of combining multiple TMPRSS2-ERG splicing isoforms as highly specific urine biomarkers for the detection of high-grade PCa.

We next used a machine learning approach to develop a prebiopsy risk predictor in a training portion of the extreme
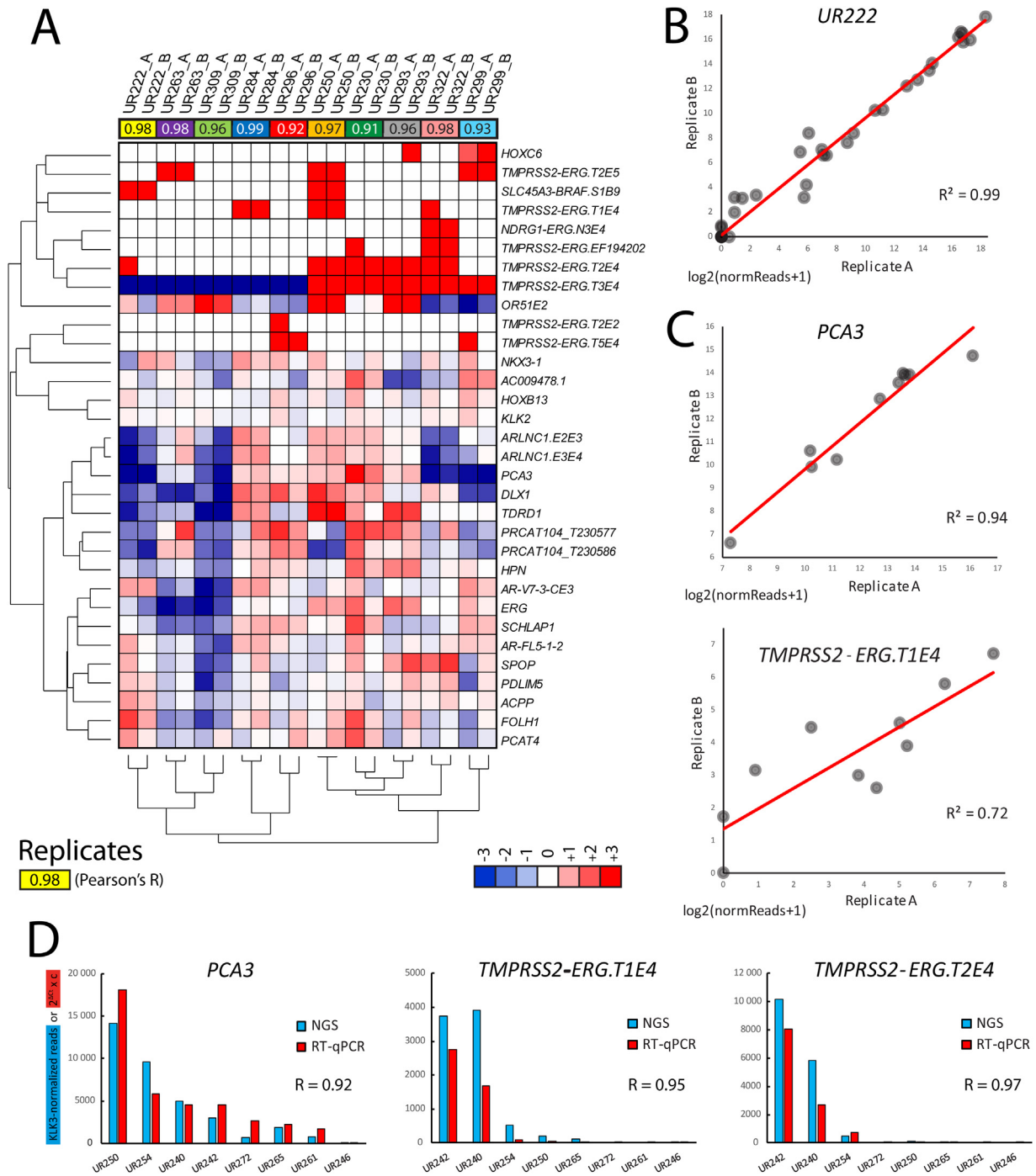
Fig. 2 – UPSeq shows high technical reproducibility and accuracy. UPSeq showed high performance in reproducibility and accuracy testing. (A) Twenty replicate NGS libraries (UR_A vs UR_B in sample ID) for ten randomly selected PCa patients' urine RNA samples were constructed and sequenced on separate days. Paired replicates are denoted with the same color in header above heatmap. Pearson's pair-wise correlation R values for all KLK3-normalized targets are shown inside colored boxes and demonstrated high reproducibility (median R = 0.97, range 0.91–0.99). Heatmap shows expression levels (gene median centered, log2[normalized reads + 1]), where red and blue indicate over- and underexpression, respectively. Gene fusion targets are restricted to those having >32 normalized sequencing reads in at least one sample (read levels below that threshold are zeroed as background noise). Unsupervised hierarchical clustering (uncentered correlation similarity metric and centroid linkage clustering method) assigned paired replicates adjacent to each other and in separate branches for all ten samples (sample dendrogram). (B) Expression levels (Log2[normalized reads + 1]) over all 84 transcripts for replicate A versus B are plotted for one representative sample (UR222) showing high concordance over the entire range of expression. (C) Expression levels (Log2[normalized reads + 1]) over all ten samples for replicate A versus B are plotted for PCA3 and TMPRSS2-ERG isoform T1E4 (targets that are part of the MiPS test) showing high concordance. (D) Assay accuracy against an orthogonal method was assessed by comparing UPSeq versus RT-qPCR in eight samples for PCA3 and the two main TMPRSS2-ERG splice isoforms T1E4 and T2E4. Bar graphs show KLK3-normalized reads for UPSeq and $2^{\Delta Ct} \times c$ for RT-qPCR (where the constant c = 30 000, 100 000, and 500 000 for PCA3, TMPRSS2-ERG.T1E4, and TMPRSS2-ERG.T2E4, respectively, for ease of visualization). Samples are sorted left to right by the RT-qPCR value. Pearson's R values are shown, demonstrating high concordance between the two orthogonal methods for all three transcripts. MiPS = Michigan Prostate Score; NGS = next-generation sequencing; PCa = prostate cancer; RT-qPCR = reverse transcription quantitative polymerase chain reaction; UPSeq = Urine Prostate Seq.
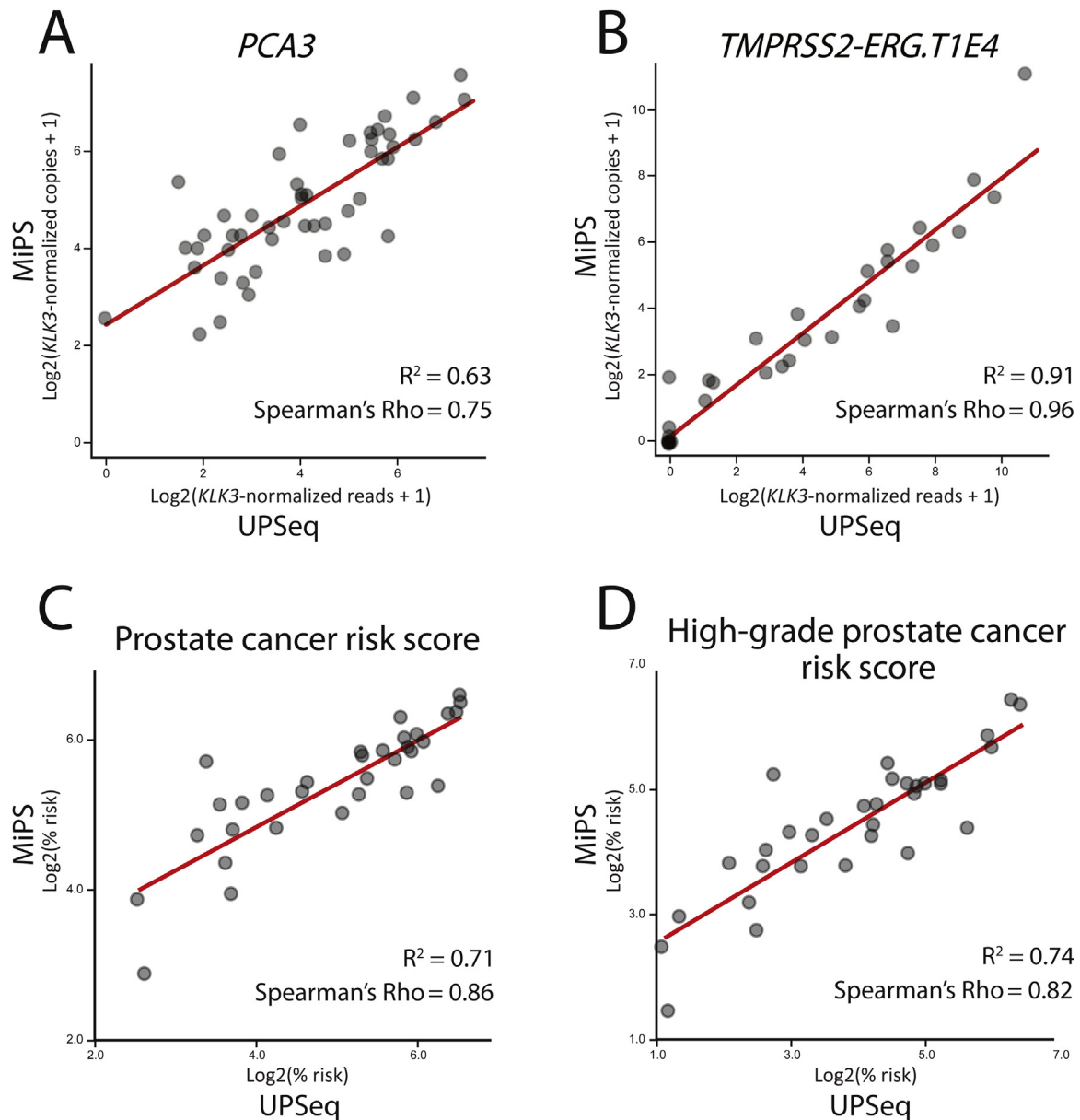
Fig. 3 – UPSeq shows high accuracy compared with the clinical MiPS laboratory developed test. We performed UPSeq on RNA isolated from stored aliquots of same urine void from PCa patients who had undergone our laboratory developed transcription-mediated amplification (TMA)-based MiPS test (measuring *PCA3* and *TMPRSS2-ERG.T1E4*). (A) For MiPS scores, clinical TMA-based *PCA3* number of copies is normalized to sample-specific *KLK3* number of copies and multiplied by a coefficient of 1000. Similarly, for UPSeq-derived scores, *PCA3* sequencing reads were normalized to sample-specific *KLK3* reads and multiplied by 1000. Expression level (Log2[normalized number of copies or sequencing reads + 1]) are plotted for 48 samples with available clinical MiPS (or PROGENSA) *PCA3* data. *PCA3* scores were highly concordant between the two methods (Spearman's rho = 0.75, linear fit $R^2 = 0.63$). (B) *TMPRSS2-ERG.T1E4* scores for the two methods were calculated and plotted as for *PCA3* in Fig. 3A (with the exception that a coefficient of 100 000 is used as opposed to 1000) for 32 samples with available clinical MiPS *TMPRSS2-ERG.T1E4* data. *TMPRSS2-ERG.T1E4* scores were highly concordant between the two methods (Spearman's rho = 0.96, linear fit $R^2 = 0.91$). Concordance plots of urine-based risk probabilities for the presence of (C) PCa and (D) high-grade PCa (grade group >1) on biopsy. The clinical MiPS algorithm [19], which combines serum PSA with urine *PCA3* and *TMPRSS2-ERG.T1E4* into a model validated to predict biopsy pathology, was used to calculate risk probabilities for clinical (TMA) and NGS-derived MiPS scores for the two transcripts. Log2(% risk) is plotted for the 32 samples having clinical MiPS data. Risk predictions were highly concordant between the two methods (Spearman's rho = 0.86 and linear fit $R^2 = 0.71$ for all-grade PCa; Spearman's rho = 0.82 and linear fit $R^2 = 0.74$ for high-grade PCa). MiPS = Michigan Prostate Score; NGS = next-generation sequencing; PCa = prostate cancer; PSA = prostate-specific antigen; UPSeq = Urine Prostate Seq.

design cohort ($n = 73$). Specifically, a random forest feature-reduction process followed by logistic regression reduced the 84 UPSeq targets to 15, yielding a model that included several *TMPRSS2-ERG* splicing isoforms, additional mRNAs, lncRNAs, and other current clinical biomarkers (Supplementary Fig. 11A and 11B). ROC curves (Fig. 4C, left) were plotted for (1) serum PSA, (2) the high-grade MiPS model (NGS derived) [19], (3) a retrained NGS-derived MiPS model (limited to the three MiPS variables, but retrained on our training set), and (4) the new 15-transcript UPSeq model.
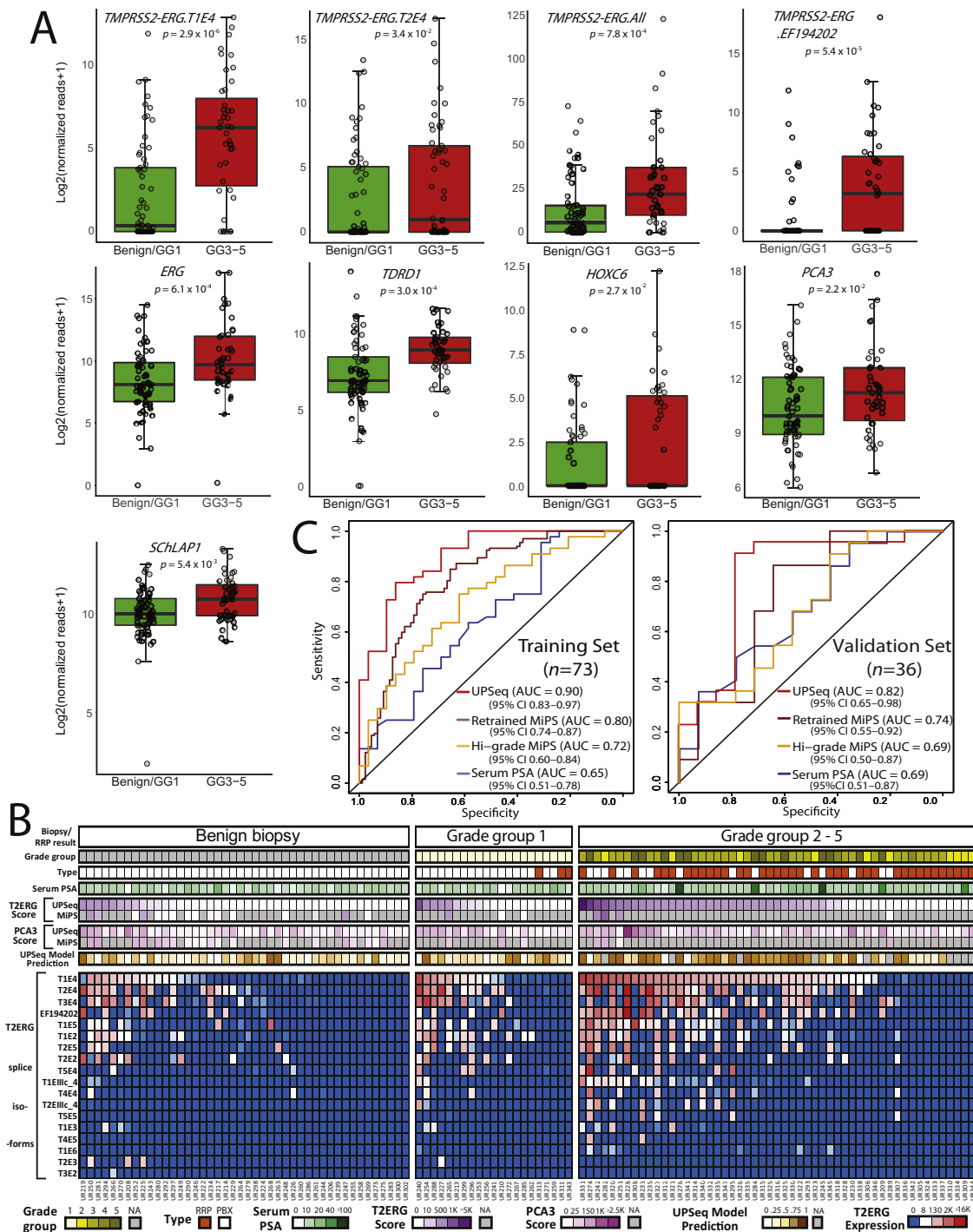
Fig. 4 – UPSeq-trained model outperforms serum PSA and derived clinical MiPS models in predicting biopsy results. Urine from a cohort of 109 patients representing those with benign or grade group (GG) 1 versus those with GG ≥3 prostate cancer (PCa) on biopsy (extreme design cohort) was subjected to the UPSeq assay. Sequencing reads for the 84 targets were normalized to sample-specific KLK3 reads and multiplied by 100 000. (A) Boxplots for nine selected targets with differential expression between the two groups are shown (median and interquartile range in log2 scale). Mann-Whitney test p values (or Student t test for normally distributed values) are shown. Boxplots for the rest of the transcripts selected in the trained UPSeq model (see below) are shown in Supplementary Figure 11. (B) Heatmap shows expression levels for all 18 targeted TMPRSS-2ERG splice isoforms (gene-median-centered, log2[normalized reads + 1]). Red and blue indicate over- and under-expression, respectively. Headers show tissue pathology results, type of tissue (RRP and PBX), serum PSA (ng/ml), clinical (TMA) and NGS-derived MiPS TMPRSS-ERG.T1E4 and PCA3 scores (calculated as in Fig. 3), and the UPSeq model (see below) prediction score from 0 to 1 for having GG ≥3 PCa on biopsy. (C) UPSeq data for all 84 targets from 73/109 extreme design cohort patients (training set), randomly selected to have a group-wise ratio proportional to that of the entire cohort, underwent a random forest target reduction method to select the minimal number of the most informative targets (29 transcripts). A regularized logistic regression model was built on the training set, which showed a higher area under the receiver operating characteristic curve (AUC = 0.9) than serum PSA or the clinical high-grade (Hi-grade), and a retrained MiPS model using derived UPSeq PCA3 and TMPRSS2-ERG.T1E4 scores (left panel). The UPSeq model also outperformed these three models in the held out set of 36 samples (validation set; AUC = 0.82; right panel). AUC 95% CIs are shown. CI = confidence interval; MiPS = Michigan Prostate Score; NGS = next-generation sequencing; PBX = prostate biopsy; PCa = prostate cancer; PSA = prostate-specific antigen; RRP = radical retropubic prostatectomy; TMA = transcription-mediated amplification; UPSeq = Urine Prostate Seq.

Expectedly, serum PSA showed the poorest discriminatory ability (AUC [95% CI] = 0.65 [0.51–0.78]), followed by high-grade and retrained MiPS models (0.72 [0.60–0.84] and 0.80 [0.74–0.87], respectively), confirming MiPS biomarker and model superiority to serum PSA alone [19]. Our new UPSeq model had the highest training-set AUC of 0.90 (0.83–0.97). Importantly, similar results were observed in the validation set ($n = 36$) where serum PSA, high grade, and retrained MiPS had AUCs of 0.69 (0.51–0.87), 0.69 (0.50–0.87), and 0.74 (0.55–0.92), respectively. The UPSeq model had the strongest performance (AUC = 0.82 [0.65–0.98]) in the validation set, supporting the potential value of additional urine biomarkers beyond PCA3 and TMPRSS2-ERG.T1E4 in early detection of PCa (Fig. 4C, right).

In exploratory analyses (see the Supplementary material for details), we retrained NGS-derived HOXC6+DLX1 (SelectMDx) [16] and PCA3+ERG (ExoDx Prostate Intelli-Score) [17] models. UPSeq model AUCs were higher than those of the HOXC6+DLX1 and PCA3+ERG models in both training and validation sets (training: 0.90 [0.83–0.97] vs 0.69 [0.57–0.81] and 0.69 [0.57–0.81], respectively; validation: 0.82 [0.65–0.98] vs 0.50 [0.50–0.50] and 0.66 [0.47–0.85], respectively; Supplementary Fig. 12).

Taken together, our results demonstrate improved performance of a multiplex biomarker approach compared with a single biomarker or a combination of a few biomarkers for detecting aggressive PCa.

4. Discussion

Here, we report the preclinical development and validation of a novel post-DRE urine-based NGS assay for the detection of aggressive PCa. Using machine learning to interrogate the expression of 84 mRNA transcripts in urine collected from men with PCa representing the ends of the disease spectrum, we developed a novel 15-transcript model that outperformed PSA, MiPS (serum PSA + urine T2:ERG + PCA3), and derived PCA3 + ERG and HOXC6 + DLX1 scores for predicting the presence of aggressive disease. These data suggest that a multiplex model can improve upon commercially available tests. Critically, to the best of our knowledge, we report for the first time the ability to detect expressed germline and somatic PCa mutations in urine RNA. Our results support the continued development and prospective clinical validation of this assay for the evaluation of men at risk of PCa.

A urine-based multiplex biomarker approach has, at least in theory, the potential to overcome tumor heterogeneity and multifocality to improve the detection of aggressive PCa. Serum PSA, a widely used PCa early detection biomarker, has led to unnecessary biopsies and overdetection of low-grade likely indolent disease (AUC = 0.59–0.64) [35]. To improve upon PSA performance, several clinically available serum- or urine-based tests comprising one to four biomarkers have been developed for aggressive PCa detection (eg, 4K [AUC = 0.78], PCA3 [AUC = 0.75], MiPS [AUC = 0.77], SelectMDx [AUC = 0.86], and IntelliScore [AUC = 0.77]) [15–17,19,36]. In the current study, our novel 15-transcript UPSeq model outperformed serum PSA, MiPS, and the derived HOXC6 + DLX1 (SelectMDx) and PCA3 + ERG (ExoDx Prostate IntelliScore) models in detecting aggressive PCa. Although for the latter two we used NGS as opposed to these assays' true method (RT-qPCR) and whole urine as opposed to IntelliScore's intended substrate (urinary exosomes), our data support the superiority of our biomarker set over currently used ones.

Our novel assay has several potential clinical applications. First, it may be useful for early detection of aggressive PCa in men undergoing initial prostate biopsy. Second, given the possible capacity to overcome tumor multifocality and heterogeneity, it has the potential to rule out high-grade disease in men considering AS or for identifying patients for surveillance biopsies. However, a formal assessment of UPSeq's predictive ability for AS upgrading and its robustness to multifocality warrants further investigation. Third, it may help identify negative MRI or benign biopsy patients, but with ongoing clinical suspicion for PCa, to undergo alternative biopsy strategies such as saturation biopsy. Lastly, the assay's ability to detect expressed germline and somatic mutations in urine presents unique opportunities for noninvasively identifying PCa familial predisposition or precision medicine approaches. Overall, our novel UPSeq assay has several potential clinical applications, and further validation studies can delineate our assay's application in those clinical scenarios.

Our study has several limitations. First, an attentive DRE is necessary prior to urine collection. Post-DRE whole urine, however, is superior to urinary sediments or exosomes for the detection of prostate/PCa-derived transcripts [37] and is the basis for the PROGENSA PCA3 [15,38], MiPS [19], and SelectMDx [16] tests. Second, our cohorts were selected in a biased manner to demonstrate the feasibility of detecting aggressive PCa transcripts in urine. Validation in larger prospective cohorts is necessary to demonstrate clinical utility. Third, our patients classified to have benign PCa had undergone prostate biopsy only and may conceivably harbor small undetected PCa foci, a known limitation of current biopsy strategies.

5. Conclusions

A urine-based liquid biopsy may help overcome PCa heterogeneity and multifocality. We developed a multiplex urine-based 15-transcript UPSeq model with improved performance for the detection of aggressive PCa. Our data support the continued development and prospective validation of this assay in larger patient cohorts for potential clinical applications in the evaluation of men at risk of PCa or aggressive PCa.

Appendix A. Supplementary data

Supplementary material related to this article can be found, in the online version, at doi:https://doi.org/10.1016/j.euo.2021.03.002.

References

[1] Stamey TA, et al. Prostate-specific antigen as a serum marker for adenocarcinoma of the prostate. N Engl J Med 1987;317:909–16.

[2] Fenton JJ, et al. Prostate-specific antigen-based screening for prostate cancer: evidence report and systematic review for the US Preventive Services Task Force. JAMA 2018;319(18):1914–31.

[3] Eggener SE, et al. A multi-institutional evaluation of active surveillance for low risk prostate cancer. J Urol 2013;189(1 Suppl):S19–25, discussion S25.

[4] Siddiqui MM, et al. Comparison of MR/ultrasound fusion-guided biopsy with ultrasound-guided biopsy for the diagnosis of prostate cancer. JAMA 2015;313:390–7.

[5] Filson CP, et al. Prostate cancer detection with magnetic resonance-ultrasound fusion biopsy: the role of systematic and targeted biopsies. Cancer 2016;122:884–92.

[6] Salami SS, et al. Biologic significance of magnetic resonance imaging invisibility in localized prostate cancer. JCO Precis Oncol 2019;3:1–12.

[7] Johnson DC, et al. Detection of individual prostate cancer foci via multiparametric magnetic resonance imaging. Eur Urol 2019;75:712–20.

[8] Raaijmakers R, et al. Complication rates and risk factors of 5802 transrectal ultrasound-guided sextant biopsies of the prostate within a population-based screening program. Urology 2002;60:826–30.

[9] Sieweke MH, Bissell MJ. The tumor-promoting effect of wounding: a possible role for TGF-beta-induced stromal alterations. Crit Rev Oncog 1994;5:297–311.

[10] Stuelten CH, et al. Acute wounds accelerate tumorigenesis by a T cell-dependent mechanism. Cancer Res 2008;68:7278–82.

[11] Loeb S, et al. Overdiagnosis and overtreatment of prostate cancer. Eur Urol 2014;65:1046–55.

[12] Mehra R, et al. Heterogeneity of TMPRSS2 gene rearrangements in multifocal prostate adenocarcinoma: molecular evidence for an independent group of diseases. Cancer Res 2007;67:7991–5.

[13] Boutros PC, et al. Spatial genomic heterogeneity within localized, multifocal prostate cancer. Nat Genet 2015;47:736–45.

[14] Palapattu GS, et al. Molecular profiling to determine clonality of serial magnetic resonance imaging/ultrasound fusion biopsies from men on active surveillance for low-risk prostate cancer. Clin Cancer Res 2017;23:985–91.

[15] Groskopf J, et al. APTIMA PCA3 molecular urine test: development of a method to aid in the diagnosis of prostate cancer. Clin Chem 2006;52:1089–95.

[16] Van Neste L, et al. Detection of high-grade prostate cancer using a urinary molecular biomarker-based risk score. Eur Urol 2016;70:740–8.

[17] McKiernan J, et al. A novel urine exosome gene expression assay to predict high-grade prostate cancer at initial biopsy. JAMA Oncol 2016;2:882–9.

[18] Tomlins SA, et al. Recurrent fusion of TMPRSS2 and ETS transcription factor genes in prostate cancer. Science 2005;310:644–8.

[19] Tomlins SA, et al. Urine TMPRSS2:ERG plus PCA3 for individualized prostate cancer risk assessment. Eur Urol 2016;70:45–53.

[20] Cancer Genome Atlas Research Network. The molecular taxonomy of primary prostate cancer. Cell 2015;163:1011–25.

[21] Grasso CS, et al. The mutational landscape of lethal castration-resistant prostate cancer. Nature 2012;487:239–43.

[22] Roychowdhury S, Chinnaiyan AM. Translating cancer genomes and transcriptomes for precision oncology. CA Cancer J Clin 2016;66:75–88.

[23] Bostrom PJ, et al. Genomic predictors of outcome in prostate cancer. Eur Urol 2015;68:1033–44.

[24] Salami SS, et al. Transcriptomic heterogeneity in multifocal prostate cancer. JCI Insight 2018;3:e123468.

[25] Hovelson DH, et al. Targeted DNA and RNA sequencing of paired urothelial and squamous bladder cancers reveals discordant geno-

mic and transcriptomic events and unique therapeutic implications. Eur Urol 2018;74:741–53.

[26] Hovelson DH, et al. Development and validation of a scalable next-generation sequencing system for assessing relevant somatic variants in solid tumors. Neoplasia 2015;17:385–99.

[27] Cani AK, et al. Next-gen sequencing exposes frequent MED12 mutations and actionable therapeutic targets in phyllodes tumors. Mol Cancer Res 2015;13:613–9.

[28] Cani AK, et al. Comprehensive genomic profiling of orbital and ocular adnexal lymphomas identifies frequent alterations in MYD88 and chromatin modifiers: new routes to targeted therapies. Mod Pathol 2016;29:685–97.

[29] Cani AK, et al. Next generation sequencing of vitreoretinal lymphomas from small-volume intraocular liquid biopsies: new routes to targeted therapies. Oncotarget 2017;8:7989–98.

[30] Paoletti C, et al. Comprehensive mutation and copy number profiling in archived circulating breast cancer tumor cells documents heterogeneous resistance mechanisms. Cancer Res 2018;78:1110–22.

[31] Ewing CM, et al. Germline mutations in HOXB13 and prostate-cancer risk. N Engl J Med 2012;366:141–9.

[32] Smith SC, et al. HOXB13 G84E-related familial prostate cancers: a clinical, histologic, and molecular survey. Am J Surg Pathol 2014;38:615–26.

[33] Niknafs YS, et al. MiPanda: a resource for analyzing and visualizing next-generation sequencing transcriptomics data. Neoplasia 2018;20:1144–9.

[34] Prensner JR, et al. The long noncoding RNA SChLAP1 promotes aggressive prostate cancer and antagonizes the SWI/SNF complex. Nat Genet 2013;45:1392–8.

[35] Martin RM, et al. Effect of a low-intensity PSA-based screening intervention on prostate cancer mortality: the CAP randomized clinical trial. JAMA 2018;319:883–95.

[36] Vickers A, et al. Reducing unnecessary biopsy during prostate cancer screening using a four-kallikrein panel: an independent replication. J Clin Oncol 2010;28:2493–8.

[37] Hendriks RJ, et al. Comparative analysis of prostate cancer specific biomarkers PCA3 and ERG in whole urine, urinary sediments and exosomes. Clin Chem Lab Med 2016;54:483–92.

[38] Auprich M, et al. Contemporary role of prostate cancer antigen 3 in the management of prostate cancer. Eur Urol 2011;60:1045–54.